D

THERMOMAGNETIC PROPERTIES OF RED SEDIMENTS

by

P. Adrian Camfield

B.Sc. (Eng.) Queen's University
(1964)

Submitted in partial fulfillment
of the requirements for the degree of

Master of Science

at the
Massachusetts Institute of Technology

June 1966

Signature of Author . . . . . .
Department of Geology and Geophysics

Certified by . . . . . .
Professor D.W. Strangway
Thesis Supervisor

Accepted by . . . . . .
Chairman, Departmental Committee
on Graduate Students

THERMOMAGNETIC PROPERTIES OF RED SEDIMENTS

by

P. Adrian Camfield

Submitted to the Department of Geology and Geophysics, Massachusetts Institute of Technology, June 1966, in partial fulfillment of the requirements for the degree of Master of Science

Abstract

Thermomagnetic analysis, the measurement of saturation magnetization over the temperature range 20°-750°C, has been used to trace the variation in iron oxide mineral content of some red sediments. Pliocene arkosic red beds from Baja California show notable amounts of ferrimagnetic magnetite and paramagnetic biotite; Pliocene muds from the Colorado River delta are strong in the metastable ferrimagnetic maghemite. Permian and Pennsylvanian red sandstones from Colorado appear to have been enriched in antiferromagnetic hematite over other iron minerals. Oxyhydroxides of iron do not appear to be important in these rocks.

Thesis Supervisor: David W. Strangway
Title: Assistant Professor of Geophysics

Table of Contents

	page
Abstract	ii
Table of Contents	iii
List of Figures	iv
List of Tables	vi
Acknowledgements	vii
I. INTRODUCTION	1
II. IRON-BEARING MINERALS AND THEIR MAGNETIC PROPERTIES	8
III. THERMOMAGNETIC ANALYSES	23
General Comments	23
Results 1. Pleistocene Soils	26
2. Pleistocene and Pliocene Muds	28
3. Thermal Breakdown of Maghemite	30
4. Pliocene Red Beds	35
5. Oligocene and Eocene Red Beds	40
6. Permian and Pennsylvanian Red Sandstones	43
7. Thermal Breakdown of Lepidocrocite	49
IV. CONCLUSIONS AND SUGGESTIONS FOR FURTHER WORK	54
References	58
APPENDIX A: The Quartz-Spring Magnetic Balance	61
APPENDIX B: Thermomagnetic Curves	70

List of Figures

Figure No.		page
1.	Susceptibility-temperature curves for garnet and biotite	11
2.	Thermomagnetic curves for Pleistocene soils	27
3.	Thermomagnetic curves for Pleistocene mud E.B.	29
4.	Thermal breakdown of maghemite from Pliocene mud 1A	32
5.	Exponential decay of maghemite at 360°C	34
6.	Thermomagnetic curves for Pliocene red bed PE 182	37
7.	Thermomagnetic curves for Oligocene red bed S-A	41
8.	Thermomagnetic curves for Eocene red bed FWBC	42
9.	Thermomagnetic curves for Permian red sandstone Fountain DP 250.2E	45
10.	Thermomagnetic curves for Permian red sandstone Lyons 6M 282.5-2	47
11.	Thermomagnetic curve for lepidocrocite	50
12.	Quartz-spring magnetic balance	64
13.	Spatial variation of electromagnet field	67
14.	Calibration of magnetic balance using substances with known Curie temperatures	69
Further thermomagnetic curves:		
15.	Pliocene mud : 1A	72
16.	Pliocene mud : SF 34	73

17.	Pliocene red bed : PE 13	74
18.	Pliocene red bed : PE 70	75
19.	Pliocene red bed : PE 270	76
20.	Pliocene red bed : PE 408	77
21.	Pliocene red bed : PE 452	78
22.	Pliocene red bed : PE 523	79
23.	Pliocene red bed : PC 27	80
24.	Pliocene red bed : WF-RB-4	81
25.	Permian red sandstone : Lykins 6M LK770-1E	82
26.	Permian red sandstone : Lykins LHR LK3	83
27.	Permian red sandstone : Lyons RMA 9891	84
28.	Permian red sandstone : Ingleside DP E-2-0	85
29.	Permian red sandstone : Fountain FF 75-1	86
30.	Pennsylvanian red sandstone : Minturn RSC 880.2	87

List of Tables

		page
Table I.	Samples analysed thermomagnetically	24
Table II.	Decrease in room-temperature magnetization of Pliocene arkoses after heating, as a percentage of initial magnetization	39
Table III.	Decrease in room-temperature magnetization of Permian and Pennsylvanian red sandstones after heating, as a percentage of initial magnetization	48

Acknowledgements

I am greatly indebted to Professor David Strangway for his guidance and encouragement in this project, and to Dr. Edwin Larson for his practical help and instruction. My thanks must also go to Professor J.R. Walker for samples of young red beds, and to Dr. Beverly McMahon for measured samples of Permian and Pennsylvanian red beds. Myron Goldstein and Dave Enggren kept me sane during long hours at the magnetic balance.

This work has been supported by the National Science Foundation, partly under the U.S.-Japan Cooperative Science Program (Grant GF-206), but mainly under Grant GP-5341.

I. INTRODUCTION

Red sediments of a variety of geologic ages from many continents have been sampled in recent years to provide information on the shape of the earth's magnetic field in the past; Collinson (1965a) lists more than fifty examples of such work. Two assumptions must be made in taking the present-day direction of magnetization of a red sediment (or of any other kind of rock) as representing the direction of the ancient geomagnetic field: first, the main component of magnetization must have been acquired in a direction essentially parallel to that field and at the time of deposition or at some recognizable time thereafter, and second, no major changes in magnetization must have taken place since that time. Minor changes of a geologic nature, such as simple folding, can be compensated for if the structure is known; minor magnetic changes, such as low-coercivity secondary magnetization, can be removed by alternating-field or thermal demagnetization.

Red sediments meet the requirements of the second assumption remarkably well. Their common occurrence in

relatively well-bedded, little-disturbed strata can make their geologic history since formation discernible, and their stability under thermal and alternating-field demagnetization suggests that their magnetization has changed very little since acquisition.

The first assumption, the contemporaneity of acquisition of magnetization and rock formation, is, however, still very much open to question. On the one hand, work such as that by Opdyke (1961), which showed excellent consistency of magnetic directions in red sediments, dolerite intrusions and basalt flows of Triassic age in New Jersey, would indicate that red sediments can become stably magnetized in the direction of the earth's field at the time of their deposition or soon after. On the other hand, red sediments have been found with directions of magnetization acquired after deposition (Helsley 1964) or after deposition and folding (Collinson 1965b), certainly well after the time of formation.

These two apparently conflicting lines of evidence point directly to the two accepted modes of magnetization of red sediments (depositional and chemical) and to the two main

ways in which iron minerals are found in them. Iron oxides occur as black crystalline grains in the sediments; together with iron hydroxides they also coat the quartz and feldspar grains to give the red beds their characteristic coloration. Some of the black crystalline grains, if originally highly-magnetic magnetite or maghemite, may have been coherently aligned in the earth's field at the time of the sediment's deposition, giving it a depositional remanent magnetization (DRM); this process was first shown to be important in varved silts by Ising (1943). Collinson's (1965c) analysis shows that "the importance of DRM in sediments will depend both on the size of the particles present and the intensity of their magnetization". King and Rees (1966) suggest, on examining limited theoretical and experimental evidence, that DRM "is not likely to be important in a sediment whose magnetic particles are less than 0.1μ or greater than 50μ or so in diameter", smaller particles being randomly oriented by Brownian motion and larger particles being too large to be oriented by the earth's field. Depositional remanent magnetization, then, is one way in which red

sediments with magnetic particles of an appropriate size range may acquire a stable magnetization at the time of formation.

The iron minerals, hematite and various iron hydroxides, which stain the sediments red, were once thought to be of detrital origin (Kyrnine 1950), but the scarcity of hematite in source areas, plus other field evidence (T.R. Walker, personal communication) indicates that the stain has formed in place (authigenically) by chemical breakdown of iron-bearing minerals - perhaps the black crystalline grains mentioned above but more likely the ferromagnesian silicates (hornblendes, biotites, etc.). Polished-section observation of some Pliocene red beds from Baja California has shown hematite growing along the cleavage planes of biotite and also forming in the black crystalline grains either as thick haoles around the original magnetite or as a complete replacement of the magnetite. Both these types of alteration could give the sediment a chemical remanent magnetization (CRM); in the case of alteration of the crystalline grains, the direction of magnetization of the hematite could be parallel

either to that of the original magnetite or maghemite or to the geomagnetic field ambient during the alteration.

The theory of the effect of authigenic chemical alteration on the direction of magnetization of a particle is not well developed. If the alteration is oxidation of magnetite to maghemite, it is possible that no change of direction occurs, since these minerals have inverse spinel crystal structures of a similar size; the short-range ordering forces found on a crystalline scale would be much stronger than the ambient geomagnetic field. E.E. Larson (personal communication), working with impure maghemites formed by oxidation of titanomagnetites in basaltic lavas, suggests that this might be the case.

If the alteration is oxidation of magnetite or maghemite to hematite, however, there is a greater probability that the geomagnetic field might influence the direction of magnetization of the material, since the rhombohedral structure of hematite is considerably different from the inverse spinel of magnetite and maghemite. If so, the magnetization of the rock would not reflect the direction of the field at the time of deposition.

The magnetic character of the fine-grained red stain may be considered as having three definite stages during the stain's growth (Irving 1964, p. 29; Kobayashi 1962). When the grains are very small, with diameters perhaps a few tens of Ångstrom units (Creer 1961), they behave superparamagnetically, possessing no stable CRM. On increasing to several hundred Å in size they become single-domain particles with a high-stability remanent magnetization in the direction of the field existing when they reach the critical blocking size (Néel 1955). With further growth the particles show multi-domain behavior, with a lower stability of remanence. This red-stain growth process must take place after the sediment's deposition.

Thus, the stable natural remanent magnetization of red sediments can be due either to depositional or to chemical processes or to both, the relative importance of either varying in each individual case. Nagata (1961, p. 213) cites work indicating that the black crystalline grains, perhaps the source of DRM, contribute relatively little to the total remanence of some red beds, while Collinson (1966),

from chemical demagnetization dissolving with acid the red pigment of other red beds, feels that the black grains can be important carriers of remanence.

With these ideas in mind, it was thought worth-while to examine the magnetic properties of minerals in some young Plio-Pleistocene red beds and to compare them with minerals found in older Permian red sandstones. This thesis presents the results of thermomagnetic, saturation magnetization-temperature, experiments on young rocks from Baja California and on older rocks from Colorado.

II. IRON-BEARING MINERALS AND THEIR MAGNETIC PROPERTIES

Since the work reported in this thesis is based on an examination of the saturation magnetization-temperature relationships for minerals contained in red sediments, a review of the known magnetic properties of relevant iron-bearing minerals is in order. The magnetic behavior of a mineral depends basically on the magnitude of the magnetic moments of the atoms which form it and on the degree of interaction between the moments. The atomic moment itself is a vector sum of electron orbital and electron spin moments; in the iron atom, which has four unpaired spins in the neutral state, the orbital moment makes a relatively minor contribution.

Diamagnetism is the simplest form of action of an applied external field on a mineral; it is, in effect, the precession of electron orbital moments about the applied field, resulting in a small negative susceptibility. Diamagnetism is evident in quartz and feldspars; it is present in all minerals, but is generally masked by stronger effects.

Paramagnetism is observed when a magnetic field is applied to an assemblage of atoms with isolated (non-inter-

acting) net moments which in zero field are randomly aligned. Application of a field H produces, in a substance containing N atoms per mol each with a net moment μ, a magnetization M per mol given in the classical limit by

$$\frac{M}{M_0} = L_\infty(a) = \coth a - \frac{1}{a} \qquad (1)$$

where $L_\infty(a)$ is the Langevin function, and

$$M_0 = N\mu, \qquad a = \frac{\mu H}{kT} \qquad (2)$$

T being the absolute temperature and k the Boltzmann constant. For $a \ll 1$, as in a weak field at high temperature,

$$\frac{M}{M_0} \approx \frac{a}{3} = \frac{\mu H}{3kT} \qquad (3)$$

so that the paramagnetic susceptibility per mol is

$$\chi_{mol} = \frac{M}{H} = \frac{N\mu^2}{3kT} \propto \frac{1}{T} \qquad (4)$$

This is the Curie law, stating that the positive susceptibility of a paramagnetic material is inversely proportional to the absolute temperature.

Ferromagnesian silicate minerals such as olivines, pyroxenes, garnets, biotites and amphiboles are typically paramagnetic. Figure 1 shows measured curves of susceptibility against temperature for a garnet from the Gatineau Hills of Québec and for biotite picked from a Pliocene red bed from Baja California. These both show the characteristic 1/T dependence of the susceptibility of a paramagnetic material.

It may be noted that the susceptibility of the biotite at a given temperature generally has a lower value when measured with decreasing temperature than with increasing temperature; the room-temperature susceptibility has decreased by 15% after heating. Nagata (1961, p. 78) states that observed susceptibility values for ferromagnesian silicates containing water, such as biotite, are "appreciably larger than the theoretical values"; perhaps the water has been driven off in the heating, causing a decrease in susceptibility. The cooling curve shows irregularities not apparent in the

FIG. 1

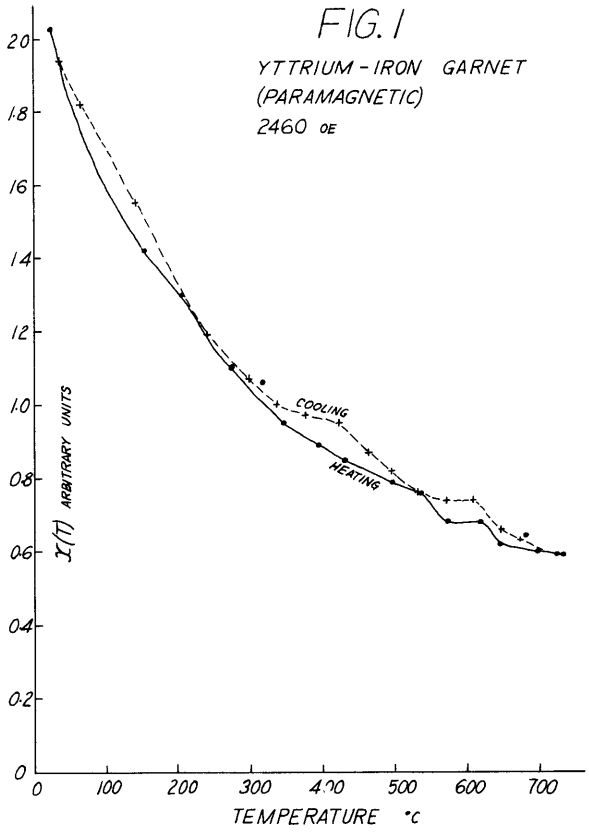
YTTRIUM - IRON GARNET
(PARAMAGNETIC)
2460 oE
20
1.8
1.6
1.4
1.2
1.0
0.8
0.6
0.4
0.2
0
χ(T) ARBITRARY UNITS
COOLING
HEATING
0
100
200
300
400
500
600
700
TEMPERATURE °C

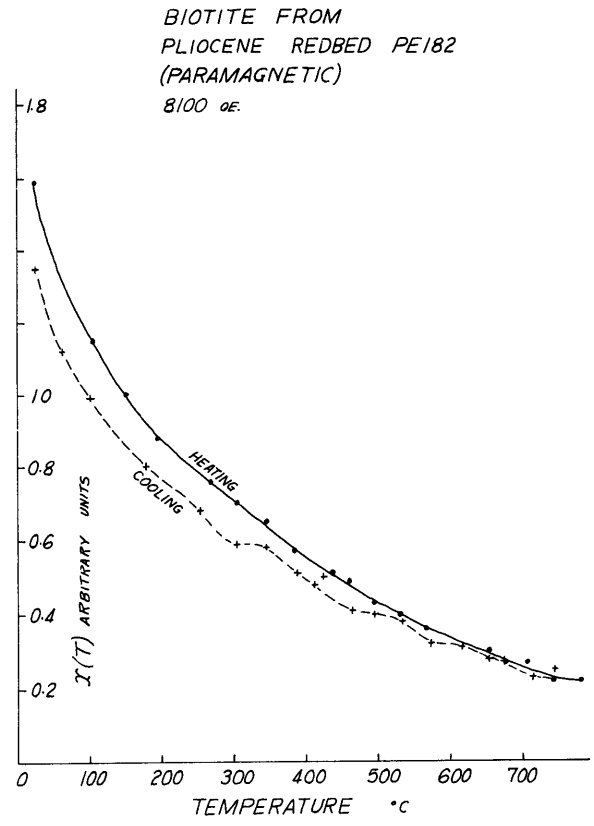
BIOTITE FROM
PLIOCENE REDBED PE182
(PARAMAGNETIC)
8100 oE.
1.8
1.0
0.8
0.6
0.4
0.2
χ(T) ARBITRARY UNITS
HEATING
COOLING
0
100
200
300
400
500
600
700
TEMPERATURE °C

heating curve which might be interpreted as Curie points (see equation (11) below); it is speculated that a small amount of ferrimagnetic material may have formed during the heating to give this effect. Certainly some kind of physico-chemical change took place; the sample, black-colored at the beginning of the experiment, was golden after heating.

Superparamagnetism refers to the alignment in an applied field of the magnetic moments of fine grains of antiferro-magnetic or ferrimagnetic (see below) materials, producing a much stronger magnetization than the paramagnetic alignment of atomic moments. The alignment of the moments of particles below a critical size (Néel 1949) can be observed at cryogenic temperatures where thermal fluctuations are reduced; under these conditions, Creer (1961) has measured the size of superparamagnetic hematite grains as 20Å.

Ferromagnetism is found in materials structured so that there is a strong exchange interaction between atomic moments which are predominantly due to electron spin. This strong interaction was first modeled by Weiss; a molecular field with sufficient magnitude to provide the observed strong

alignment of atomic moments was introduced. The effective field, H_{eff}, acting on the moments is taken as:

$$H_{eff} = H_{app} + WJ \tag{5}$$

where H_{app} is the applied field (corrected for any demagnetizing effect), J the intensity of magnetization and W a constant. Since

$$M = \frac{A}{\rho} J \tag{6}$$

(where A is the atomic weight and ρ the density), then

$$H_{eff} = H_{app} + W\frac{\rho}{A} M \tag{7}$$

Substituting $a = \mu H_{eff}/kT$ and rearranging,

$$\frac{M}{M_o} = \frac{A}{W\rho}\left(\frac{kT}{N\mu^2} - \frac{H_{app}}{N\mu}\right) \tag{8}$$

From this expression it may be seen that M/M_o has a finite value when the applied field, H_{app}, is zero; this is the

spontaneous magnetization of a ferromagnetic, given by

$$\frac{M_{spon}}{M_0} = \frac{A}{W\rho}\,\frac{kT}{N\mu^2}\,a \tag{9}$$

Equation (3), derived for a paramagnetic, is valid in this situation at temperatures high enough that random thermal vibrations of the atoms begin to decrease the spontaneous magnetization by disrupting the aligning effect of the molecular field. There will be a temperature T_c at which the spontaneous magnetization is destroyed by the thermal action; at that point, equations (3) and (9) must be identical, requiring

$$\frac{A}{W\rho}\,\frac{kT_c}{N\mu^2} = \frac{1}{3} \tag{10}$$

or

$$T_c = \frac{1}{3}\,\frac{W\rho}{A}\,\frac{N\mu^2}{k} \tag{11}$$

T_c is the Curie temperature of a ferromagnetic.

Above the Curie temperature, the Curie law (4) must be modified:

$$\chi_{mol} = \frac{M}{H_{eff}} = \frac{M}{H_{app} + \frac{W\rho}{A} M} = \frac{N\mu^2}{3k} \frac{1}{T} \qquad (12)$$

or

$$\chi_{mol} = \frac{M}{H_{app}} = \frac{N\mu^2/3k}{T - \frac{N\mu^2}{k} \frac{W\rho}{A}} \qquad (13)$$

Using equation (11), this becomes

$$\chi_{mol} = \frac{N\mu^2/3k}{T - T_c} \propto \frac{1}{T - T_c} \qquad (14)$$

This shows that above the Curie temperature ferromagnetic materials must behave paramagnetically. Ferromagnetism is generally found in metals and metal alloys; a magnetization-temperature curve for nickel is shown in Figure 14.

The atomic ordering discussed above extends in a ferromagnetic substance over a volume with dimensions of the order of 10^{-4} cm, called a magnetic domain; the direction of magnetization in a domain in zero applied field will be the "easy" direction, where the magnetocrystalline energy due to

crystal structure anisotropy will be minimized. In general, neighboring domains will be magnetized in antiparallel senses, to minimize the magnetostatic energy of free magnetic poles; the transition zones between domains, domain walls, will have a thickness reflecting the balance of exchange energy with magnetocrystalline energy in these regions. Similarly, domain widths will adjust themselves to equalize wall energy with magnetostatic energy.

With the domain concept in mind, the effect of an increasing applied field on a ferromagnetic can be described. Initially, domains with easy directions of magnetization closest to the direction of the applied field will grow at the expense of other domains by reversible migration of domain walls. Second, there follows discontinuous, irreversible wall movement against the irregular stress distribution caused by defects, impurities, etc., in the crystal structure, until most of the remaining domains are magnetized in the same (easy) direction. Third, a further increase in applied field rotates the direction of magnetization reversibly toward the field direction, until saturation magnetization,

J_s, is reached. At this point, as implied, no further increase in magnetization is possible. The magnitude of saturation magnetization and of the field required to produce saturation is often characteristic of a given ferromagnetic material.

Antiferromagnetism is evidence of a negative exchange interaction between neighboring atoms, causing an antiparallel alignment of atomic moments. Such a structure can be visualized as two sublattices of atoms magnetized in antiparallel directions, giving the substance a zero spontaneous magnetization and an apparent paramagnetic behavior with maximum susceptibility at the Néel temperature, T_N. Above T_N the susceptibility fits this expression:

$$\chi = \frac{N\mu^2/3k}{T+\theta} \quad (T > T_N) \tag{15}$$

where θ is a constant generally positive and greater than T_N.

Ilmenite ($FeTiO_3$) is paramagnetic above liquid nitrogen temperatures but has an antiferromagnetic structure at lower temperatures, with $T_N = -205°C$. Hematite (αFe_2O_3) is also

antiferromagnetic, with the modification discussed in the next paragraph; T_N = 677°C.

Parasitic ferromagnetism is found superposed on some antiferromagnetics, and is thought to be a result of either imperfect antiparallel alignment of electron spins or ferromagnetic impurities. The magnetization, σ, of a substance showing parasitic ferromagnetism may be expressed as a function of the temperature T and the applied field H:

$$\sigma(H,T) = \sigma_o(T) + \chi(T)H \qquad (16)$$

where σ_o is the parasitic ferromagnetization and χ the antiferromagnetic susceptibility.

Hematite, with rhombohedral structure, exhibits this phenomenon; the Curie temperature of the parasitic ferromagnetism coincides with the Néel temperature of the antiferromagnetism at 677°C. In addition, there is a transition at -23°C at which the axis of the antiferromagnetic alignment changes direction and at which the parasitic ferromagnetism disappears. The room-temperature saturation magnetization

for hematite is 0.1 to 0.5 emu/g (0.5 to 2.5 emu/cm^3); a curve of the temperature variation of the saturation magnetization of hematite is shown in Figure 14.

Ferrimagnetism is found in a class of metallic oxides termed ferrites which have composition $MOFe_2O_3$, where M is a metal ion of valence two. Natural ferrites generally have magnetic properties similar to ferromagnetics, although x-ray and neutron diffraction study has shown that most have the inverse spinel configuration $Fe^{3+}(M^{2+}Fe^{3+})O_4^{2-}$, with two sublattices aligned in antiparallel directions, as in an antiferromagnetic. However, the magnetization of the two sublattices is not equal, resulting in a net spontaneous magnetization with a valid Curie temperature.

Magnetite (Fe_3O_4) has eight Fe^{3+} ions in the tetrahedral sites of one sublattice of a unit cell, and eight Fe^{3+} and eight Fe^{2+} in the octahedral sites in the other sublattice of the cell. The moments of the Fe^{3+} ions counteract each other, leaving a net magnetization due to the Fe^{2+} ions; a saturation magnetization of 92-93 emu/g (478-483 emu/cm^3) results at room temperature. The Curie point is 578°C.

Magnetite also suffers a low-temperature transition, at -160°C, from an inverse spinel to an orthorhombic structure; at -143°C the crystal is magnetically isotropic.

The room-temperature saturation magnetization and the Curie temperature of magnetite vary considerably with titanium content (Nagata 1961, pp. 89-90), with J_s values varying from 10 to 90 emu/g, and T_c from 100°C to 580°C as the chemical composition varies from 80% $TiFe_2O_4$ - 20% Fe_3O_4 to 100% Fe_3O_4. The source rocks for most of the red sediments investigated in this thesis are granitic; they have a low titanium content, and thus little change in the J_s and T_c values from those for pure magnetite was expected or found.

Maghemite (γFe_2O_3) has an inverse spinel structure like that of magnetite, allowing the two to form a complete solid solution series. One-ninth of the iron sites in maghemite are vacant, however; this is an indication of its formation from magnetite by progressive low-temperature oxidation. The room-temperature magnetization of pure maghemite is 83.5 emu/g (408 emu/cm^3), somewhat less than that of pure magnetite. Maghemite is metastable, breaking down

to hematite continuously over the temperature range 200° to 600°C, with a consequent ten-fold or greater decrease in saturation magnetization at room temperature (see Figure 4). The inversion temperature of a particular component is strongly dependent on impurity substitution (Pouillard 1950); by using Na ions as stabilizing agents, Chaudron and Michel (1938) were able to determine a Curie point for maghemite at 675°C.

Two oxyhydroxides of iron, goethite (α FeOOH) and lepidocrocite (γ FeOOH), occur naturally; on heating they dehydrate to oxides, goethite going to hematite above 400°C and lepidocrocite to maghemite above 250°C (Kulp and Trites 1951). The latter transition is accompanied by a dramatic increase in saturation magnetization (Michel and Gallissot 1937). Creer (1962) has carried out a study at cryogenic temperatures of the magnetic properties of natural and synthetic oxyhydroxides.

This summarizes the properties of the iron-bearing minerals relevant to a study of the saturation magnetization-temperature relations for red sediments: ferromagnesian silicate minerals are paramagnetic, hematite is antiferromagnetic with a parasitic ferromagnetism, and magnetite and

maghemite are ferrimagnetic, maghemite being metastable. Further details are found in Nagata (1961, chapters I and III), Irving (1964, chapter 2), Nicholls (1955) and Buddington and Lindsley (1964).

III. THERMOMAGNETIC ANALYSES

General Comments

Thermomagnetic analyses (measurements of the change of saturation magnetization or susceptibility with temperature) were run on unseparated samples, magnetic separates, and non-magnetic separates from about 25 red sediments - soils, muds, arkoses and sandstones - as detailed in Table I.

Samples were crushed and ground up in water to a particle size of a few hundred microns or less, and with the aid of a small hand magnet the strongly magnetic fraction was separated out. The magnetic separate and the non-magnetic residue were then dried at 35° - 40°C before analysis. For the magnetic separate, 10 - 15 mg of sample were usually sufficient for good readings. For the unseparated rock and the non-magnetic separate, sample size was limited by the capacity of the fused quartz sample carrier; usually about 40 mg were run.

The magnetic balance on which the J_s - T curves were taken utilized a fused quartz spring to measure the vertical force exerted on the magnetized material in a vertically

TABLE I

Samples Analysed Thermomagnetically

Age	Rock Type	Formation	Location	Number of samples
Pleistocene (less than 1 m.yr.)	soil		San Diego, Calif.	1
	soil		Hermosillo, Mexico	3
	mud		San Felipe, Mexico	1
Pliocene (1-10 m.yr.)	mud		San Felipe, Mexico	2
	arkose		Baja California, Mexico	9
Oligocene (25-40 m.yr.)	sandstone	Sespe	California	1
Eocene (40-60 m.yr.)	sandstone	Wasatch	Utah	1
Permian (225-270 m.yr.)	sandstone	Lykins	Colorado	2
		Lyons		2
		Ingleside		1
		Fountain		2
Pennsyivanian (270-310 m.yr.)	sandstone	Minturn	Colorado	1

non-uniform magnetic field, the force being proportional to the magnetization. Theory of operation and construction details are given in Appendix A. Samples were heated in air to 750°C in an electric furnace; a point where with increasing temperature the magnetization began to level off following a marked decrease was chosen as the Curie temperature of a component material.

On almost all the curves it was noticed that the value of magnetization at a given temperature when measured on the cooling cycle was smaller than the value taken during the heating cycle. It is probable that this behavior is a characteristic of the samples such as breakdown of maghemite in the magnetic separates and dehydration or other changes in the ferromagnesian silicate content of the non-magnetic separates. It seems certain that the difference on heating and cooling is not due to the technique of measurement. The small mass and consequent low thermal inertia of the sample makes it likely that the sample temperature is the same as that measured by the thermocouple 0.5 cm distant. This is indicated by the negligible differences found between readings

taken at the end of the cooling process and one taken twelve hours later. To check for changes in the spring characteristics, the direction of the force on the sample was reversed by rotating the magnet pole pieces 180°, so that when the field was applied the spring was in one case stretched and in the other case relaxed by the magnetization. Little or no difference was noted in the results from either arrangement. (On a few occasions sample particles were so magnetic that the force applied upward exceeded their weight, causing them to jump out of the sample bucket. An immediate shift in the zero-field position of the spring made this loss of material readily apparent, however, and the run was terminated.)

Results 1. Pleistocene Soils

Curves are presented in Figure 2 for the $<2\mu$ fraction (particle size less than two microns) of three unseparated samples from different levels in a bright red, friable Pleistocene soil from near Hermosillo, Mexico, and for one sample from a similar soil near San Diego, California. All show a strong paramagnetic content and a small amount of

FIG. 2

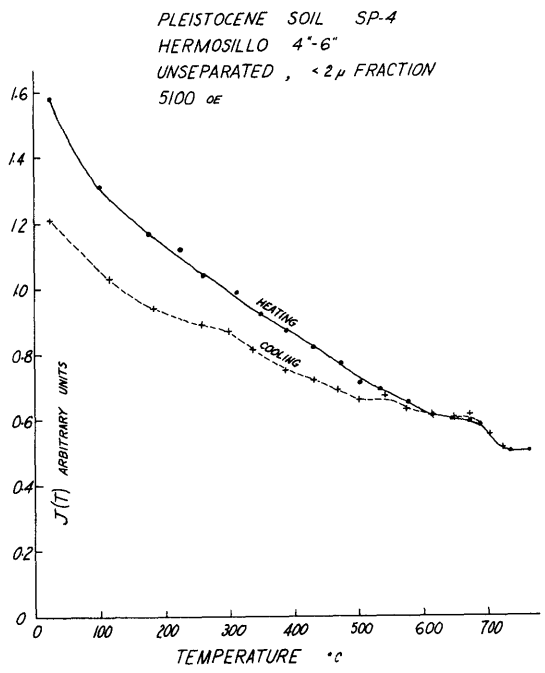
PLEISTOCENE SOIL SP-4
HERMOSILLO 4"-6"
UNSEPARATED , <2μ FRACTION
5100 oE
HEATING
COOLING
J(T) ARBITRARY UNITS
TEMPERATURE °C

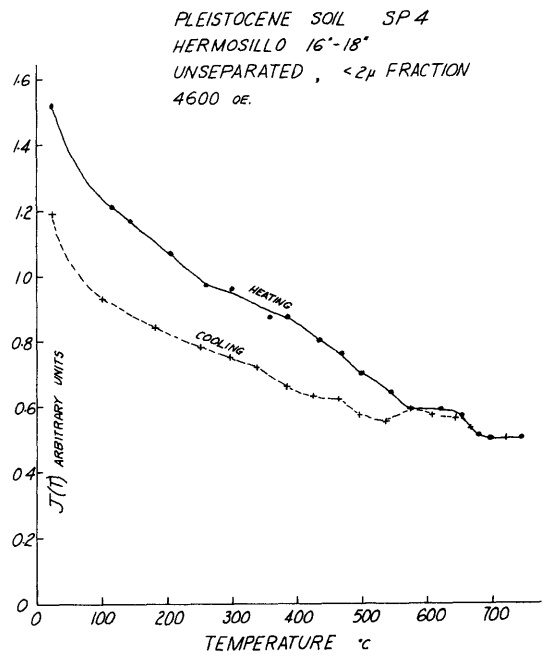
PLEISTOCENE SOIL SP 4
HERMOSILLO 16"-18"
UNSEPARATED , <2μ FRACTION
4600 oE.
HEATING
COOLING
J(T) ARBITRARY UNITS
TEMPERATURE °C

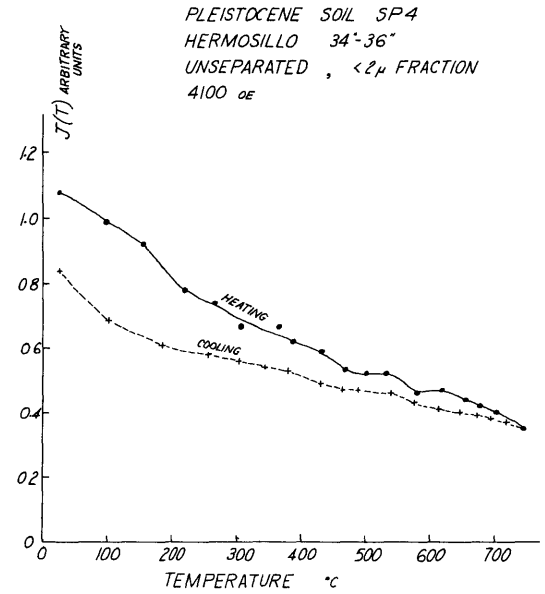
PLEISTOCENE SOIL SP4
HERMOSILLO 34"-36"
UNSEPARATED , <2μ FRACTION
4100 oE
J(T) ARBITRARY UNITS
HEATING
COOLING
TEMPERATURE °C

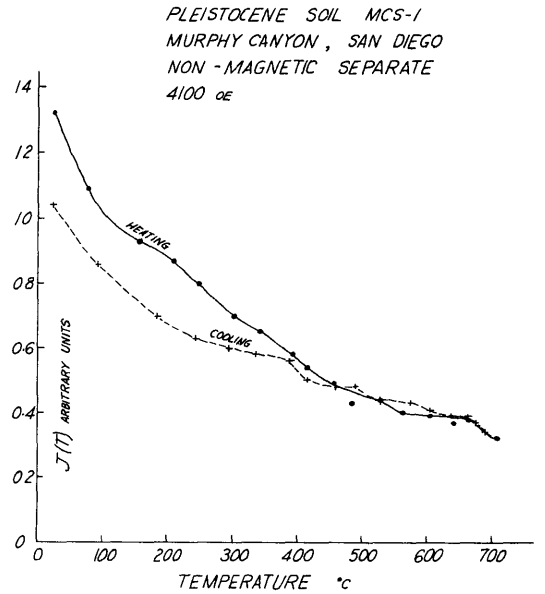
PLEISTOCENE SOIL MCS-1
MURPHY CANYON , SAN DIEGO
NON-MAGNETIC SEPARATE
4100 oE
HEATING
COOLING
J(T) ARBITRARY UNITS
TEMPERATURE °C

hematite with a Curie temperature at 680°C. The downshift of the curves during cooling is likely connected with chemical changes in the paramagnetic minerals, since the shape of the heating curves shows little recognizable maghemite content.

Results 2. Pleistocene and Pliocene Muds

Figure 3 shows typical curves for a Pleistocene mudstone deposited south of modern tidal flats at the mouth of the Colorado River. The mudstone samples came from sea cliffs on the west coast of the Gulf of California; modern muds in this region tend to be gray-colored, while Pleistocene samples are cream-brown, and Pliocene muds are banded with white and pinkish layers. The pink zones contain roughly twice as much iron as the white ones (T.R. Walker, personal communication).

The curve in Figure 3 for the unseparated mud sample E.B. can be interpreted as a combination of paramagnetic and maghemite effects. The upward bulge of the heating curve in the temperature range 100 - 400°C probably reflects the presence of maghemite, while the shape of the cooling curve (with most of the maghemite broken down) suggests paramagnetic ferromagnesian silicate material.

FIG. 3

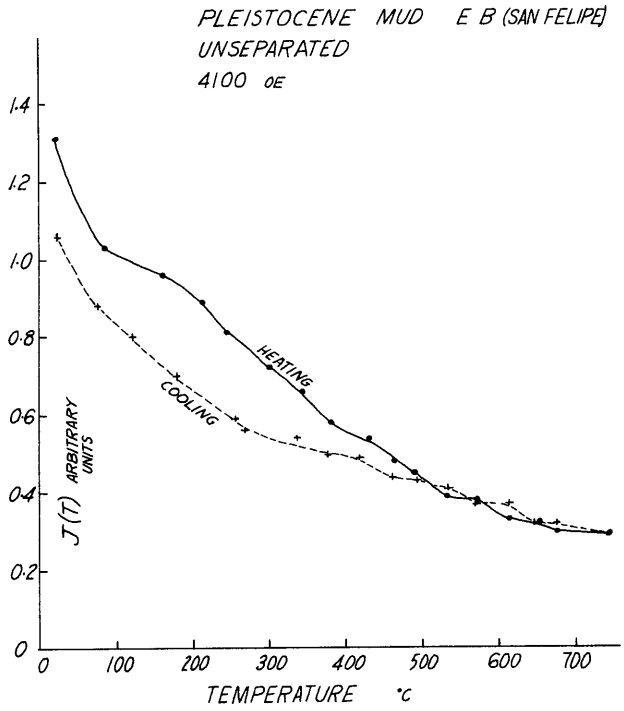
PLEISTOCENE MUD E B (SAN FELIPE)
UNSEPARATED
4100 oE
1.4
1.2
1.0
0.8
0.6
0.4
0.2
0
J(T) ARBITRARY UNITS
HEATING
COOLING
0
100
200
300
400
500
600
700
TEMPERATURE °C

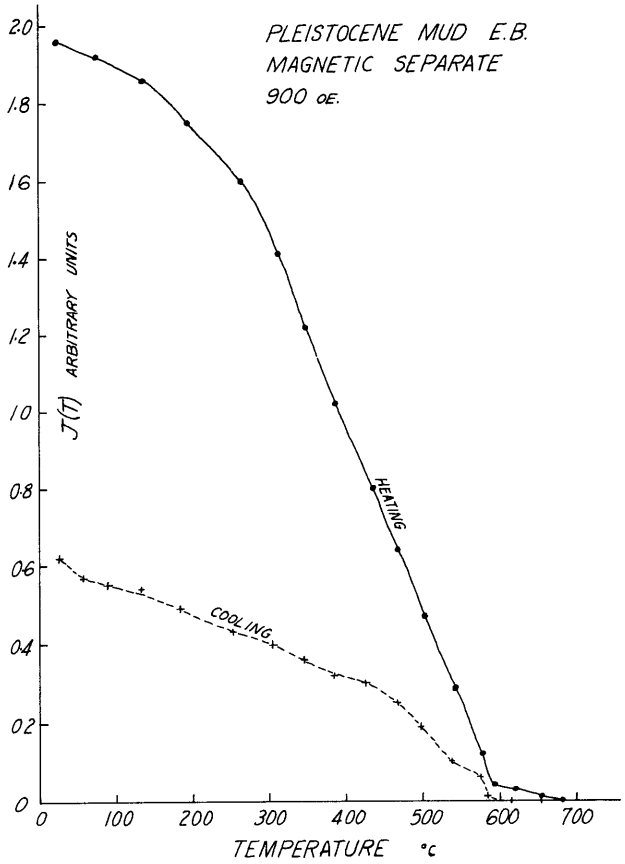
PLEISTOCENE MUD E.B.
MAGNETIC SEPARATE
900 oE.
2.0
1.8
1.6
1.4
1.2
1.0
0.8
0.6
0.4
0.2
0
J(T) ARBITRARY UNITS
HEATING
COOLING
0
100
200
300
400
500
600
700
TEMPERATURE °C

The curve for the magnetic separate, showing a 70% decrease in saturation magnetization at room temperature after heating, is a good example of the conversion of metastable maghemite to hematite over the temperature range 300° - 670°C. The cooling curve is probably that of magnetite with a Curie point at 585°C, although some maghemite, stabilized against transition by impurity content (Chaudron and Michel 1938), may yet be present, as indicated by the Curie point at 670°C on the heating curve. This Curie point might be interpreted as that for hematite, but the saturation magnetization of hematite is too small for the mineral to be detected in the relatively low field gradient applied in this run.

Results 3. Thermal Breakdown of Maghemite

To investigate the thermally-induced phase change of maghemite (γFe_2O_3) to hematite (αFe_2O_3), material was separated magnetically from a mud known to contain maghemite (see Figure 15) and treated under a modified heating program. The sample was held at constant temperature for a half hour (more or less) at each step in the heating cycle. Magnet-

ization was measured at ten-minute intervals during each constant-temperature period; within the resolution of the instrument a monotonic decrease in magnetization was observed with increasing time at constant temperature, as shown in Figure 4.

It seems reasonable to model the breakdown of maghemite at constant temperature as occurring exponentially with time, since this form of decay is common in natural systems. Let J(t) be the magnetization at time t, where t is measured from the instant the sample reaches the constant temperature T. Then, neglecting the magnetization of the hematite formed from the maghemite,

$$J(t) = J_T + J_o e^{-\lambda t} \tag{17}$$

where J_T is the magnetization of the maghemite stable at T, J_o that of the maghemite which will transform at T, and λ a decay constant. There follows:

$$\log_e \left[J(t) - J_T \right] = \log_e J_o - \lambda t \tag{18}$$

FIG. 4

MAGHEMITE BREAKDOWN IN MAGNETIC SEPARATE OF PLIOCENE MUD IA

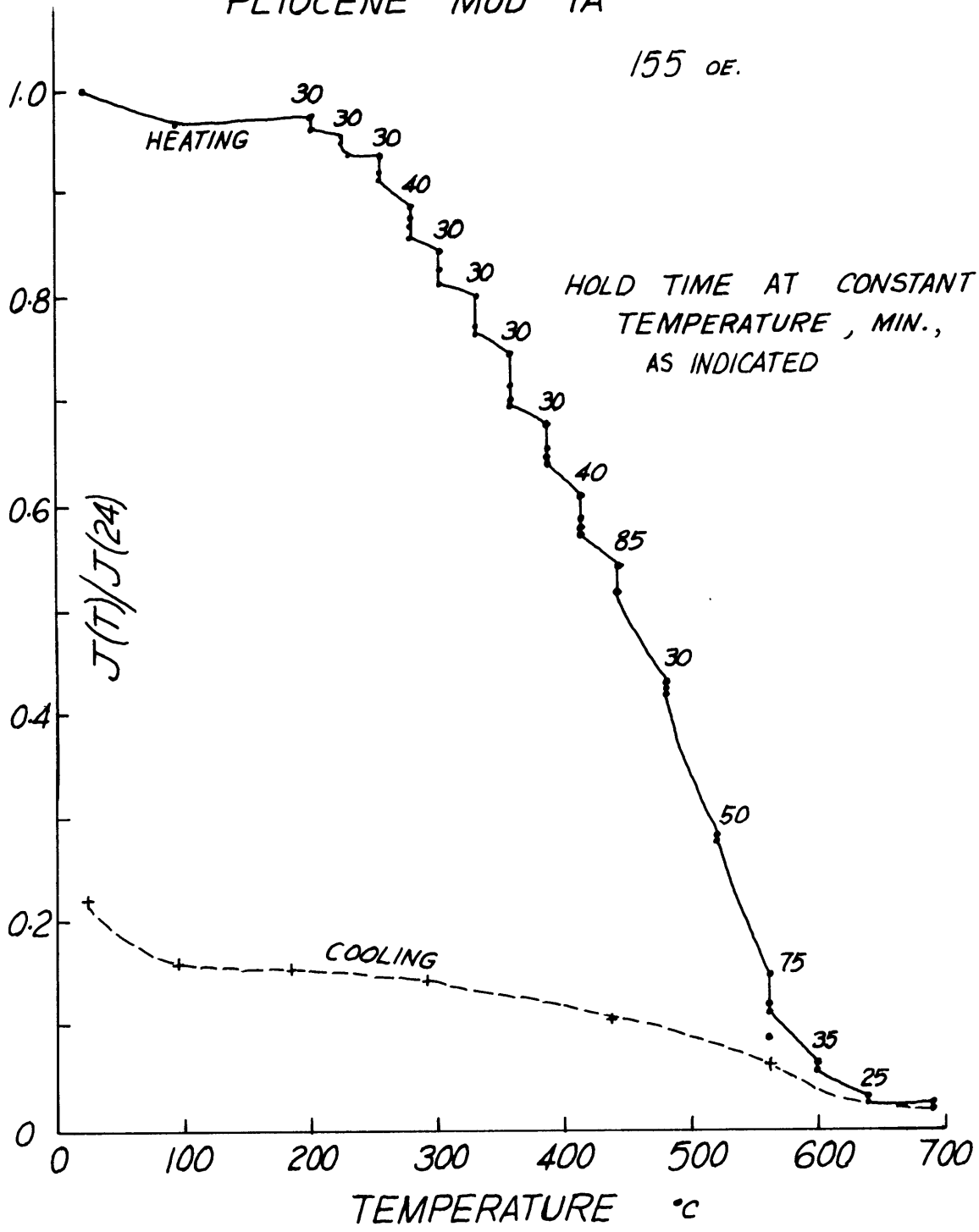

Data are plotted in semi-logarithmic form in Figure 5 for the decrease in magnetization at 360°C; the slope of the line gives 7 ± 4 min for the half-life of that fraction of the maghemite which is unstable at 360°C. Similar values of the decay parameter are associated with transformations at other temperatures above 200°C.

The experiment indicates, then, that for the maghemite in this mud there is a continuous range of breakdown temperatures from 200° to 670°C, and that at a particular temperature only a limited fraction of the material will transform. It would seem that the remaining maghemite does not change phase until the corresponding transition temperatures are reached. Pouillard (1950) has suggested that the breakdown temperature increases with impurity content, and also that the solubility in the maghemite lattice of one such impurity, alumina, is a strong function of temperature. These two suggestions, if together applicable to impurities of other such metal oxides (those of titanium, ferrous iron, etc.), might explain why some components of the maghemite heated here are stabilizied against breakdown up to relatively high temperatures.

FIG. 5

EXPONENTIAL DECAY OF MAGHEMITE AT 360 °C 155 OE.

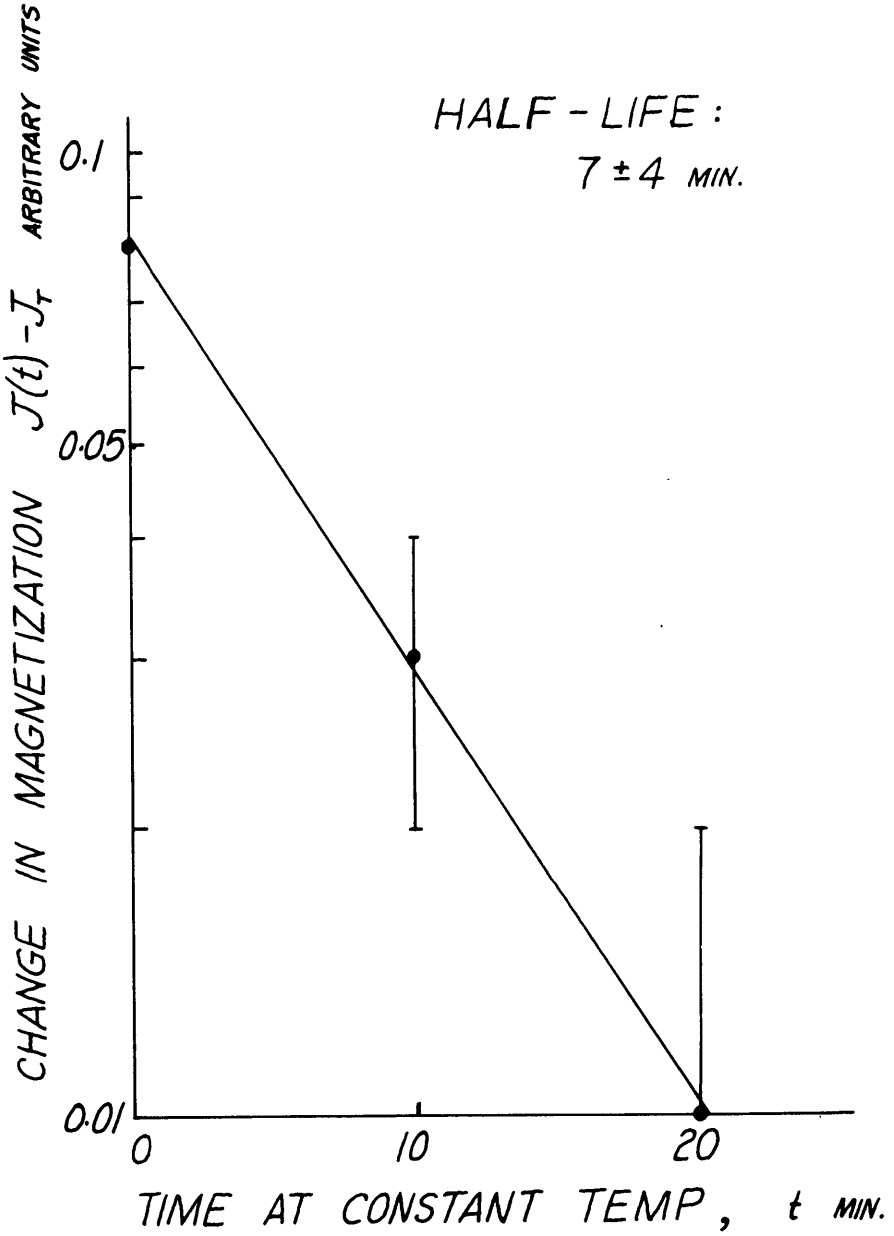

Results 4. Pliocene Red Beds

Pliocene red beds from a continuous section in Baja California were intensively investigated in this project to try and trace changes in the magnetic minerals with position in the section, i.e., with time. These rocks are arkosic, poorly-sorted and weakly-consolidated, with much unweathered granitic source rock present in sizes from fine sand to large boulders. Red material, giving the rocks their characteristic color, is found absorbed in the interstitial clay and precipitated on the surface of unweathered fragments of all sizes.

Preliminary measurements of the natural remanent magnetization of these red beds with a spinner magnetometer shows that they are very weakly magnetized, with remanent intensities of less than 5×10^{-7} emu/cm^3. Large unstable components appear to make these measurements difficult; satisfactory reproducibility was obtained only by spinning the samples in a "field-free" space where the field of Helmholtz coils reduced the earth's field to less than 1% of its value.

As mentioned in the Introduction, polished sections of these red beds were examined under reflected light with

magnifications up to 1500X. Hematite was observed as large and small detrital grains, as alteration products of magnetite, and as rod- or plate-shaped crystals in the cleavage planes of degrading biotite. Red-colored interstitial material was evident between all grains. In the samples studied optically, surfaces of the unweathered granitic fragments showed very little magnetic material present, although the yield of the magnetic separation of the whole rock was relatively high.

Generally speaking, the red beds were prepared for analysis by removing grains larger than a few millimeters in size and then crushing and separating, as discussed previously. Figure 6 shows curves for sample PE 182 from the middle of the section; similar results for other samples are presented in Appendix B.

Almost all the unseparated arkoses show strong magnetite Curie points of 575° - 590°C, and fairly good hematite with T_c values between 670° and 690°C. There is perhaps a slight suggestion of paramagnetic effects in the rather steep slope of the heating curves up to about 400°C. The downshift of the cooling curves amounts at room temperature to 10% - 20%,

FIG. 6

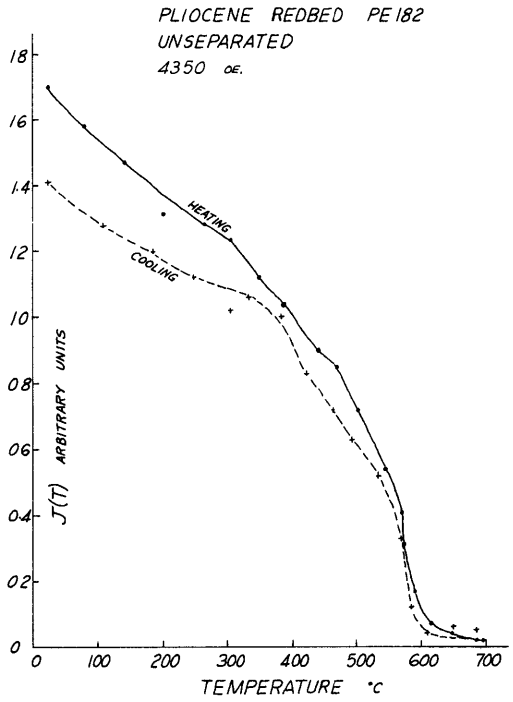
PLIOCENE REDBED PE 182
UNSEPARATED
4350 oE.
HEATING
COOLING
J(T) ARBITRARY UNITS
TEMPERATURE °C
0
0.2
0.4
0.6
0.8
1.0
1.2
1.4
1.6
1.8
0
100
200
300
400
500
600
700

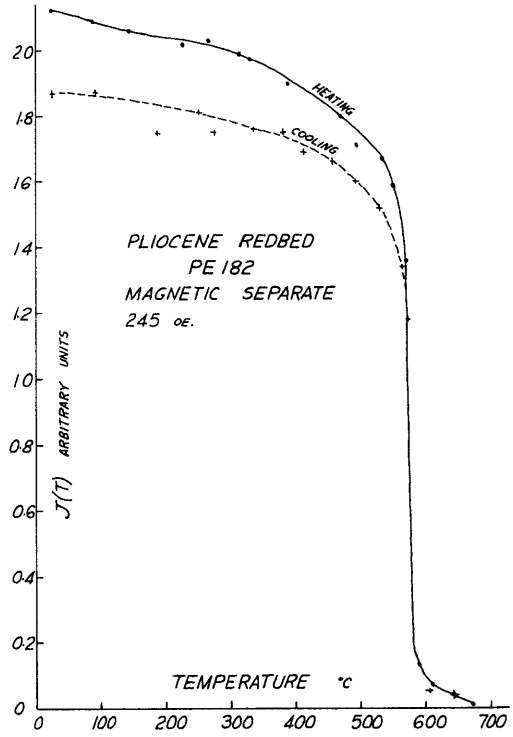
HEATING
COOLING
PLIOCENE REDBED
PE 182
MAGNETIC SEPARATE
245 oE.
J(T) ARBITRARY UNITS
TEMPERATURE °C
0
0.2
0.4
0.6
0.8
1.0
1.2
1.4
1.6
1.8
2.0
0
100
200
300
400
500
600
700

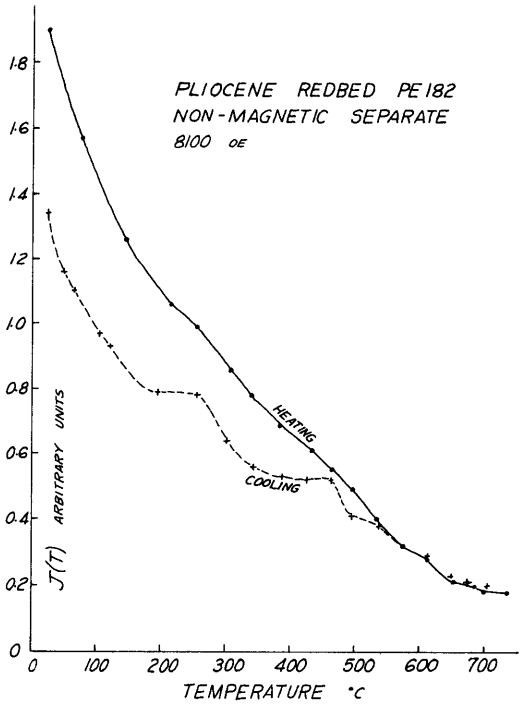
PLIOCENE REDBED PE 182
NON-MAGNETIC SEPARATE
8100 oE
HEATING
COOLING
J(T) ARBITRARY UNITS
TEMPERATURE °C
0
0.2
0.4
0.6
0.8
1.0
1.2
1.4
1.6
1.8
0
100
200
300
400
500
600
700

as shown in Table II, indicating low maghemite content. Sample PE 408, red material scraped from a weathered surface of the hand specimen, was an exception; it gave a 65% downshift, and less magnetite than most samples, although just as much hematite (see Figure 20). This is probably due to the different sample preparation.

Magnetic separates were very rich in magnetite, with "text-book" curves showing Curie temperatures at 575° - 590°C. Maghemite breakdown was low, only 10% - 20% in most samples; details are given in Table II. There is a slight pattern of increasing maghemite content with depth in the section, but it is not known whether this is significant, since there probably exists as much horizontal inhomgeneity as vertical in this location.

The character of the curves for the non-magnetic separates is distinctly paramagnetic, with evident breakdown of susceptibility through dehydration, and some hint of the formation of ferrimagnetic material during the heating, as discussed previously in the section on magnetic minerals.

TABLE II

Decrease in room-temperature magnetization of Pliocene arkoses after heating, as percentage of initial magnetization

Sample	Whole rock (maghemite and biotite breakdown)	Magnetic separate (maghemite breakdown)	Non-magnetic separate (biotite breakdown)
Top of section			
PE 523	40	24	
PE 452	17	10	15
PE 408	65	-15*	
PE 270	13	2	14
PE 182	17	12	29
PE 70	31	20	21
PE 13	22	43	20
Bottom of section			

*Magnetization increased after heating; this sample alone was heated in vacuum.

Results 5. Oligocene and Eocene Red Beds

Results for two red beds of Oligocene and Eocene ages are presented in Figures 7 and 8. Some of the curves are rather nondescript, but a few have features worth discussing.

The unseparated Oligocene sample of Figure 7 has a 50% maghemite downshift, as does the magnetic separate. In addition, the cooling curve of the magnetic separate shows magnetite (585°C), hematite (680°C), and probably an iron impurity (780°C) which is partially altered by heating, as reflected by the breakdown on cooling between 780° and 680°C. The non-magnetic separate is paramagnetic.

The magnetic separate of the Eocene red bed (Figure 8) shows magnetite through Curie points at 587°C on heating and at 595°C on cooling. Also, maghemite is present; evidence for this is a Curie point at 680°C followed by substantial breakdown of saturation magnetization. The curve for the fine-grained part of the non-magnetic separate, red-colored, almost colloidal in particle size, is dominated by a hematite Curie point at 680°C; no paramagnetic material can be seen. A featureless curve for the unseparated material, plus the

FIG. 7

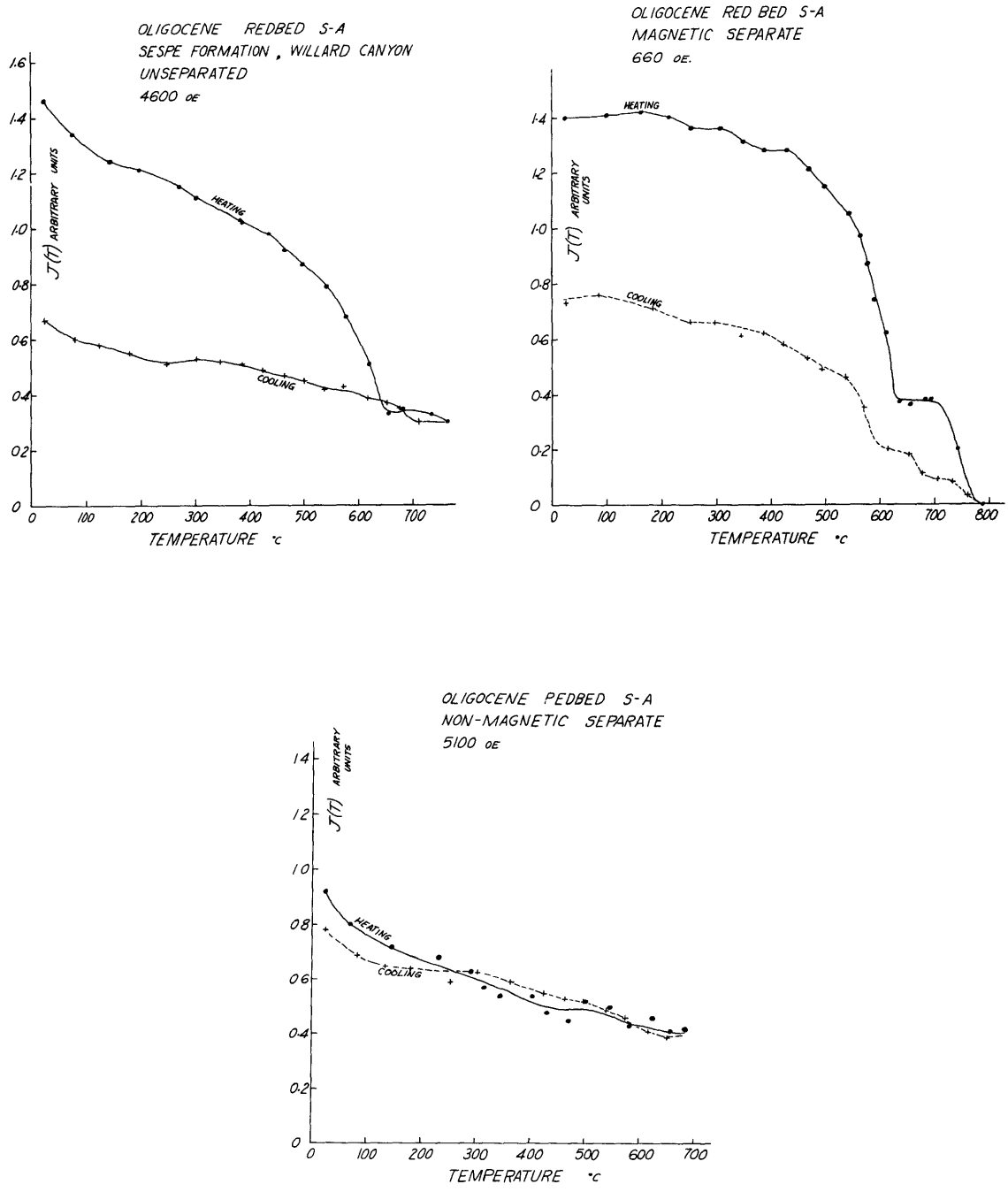
OLIGOCENE REDBED S-A
SESPE FORMATION, WILLARD CANYON
UNSEPARATED
4600 oE
J(T) ARBITRARY UNITS
HEATING
COOLING
TEMPERATURE °C
OLIGOCENE RED BED S-A
MAGNETIC SEPARATE
660 oE.
OLIGOCENE PEDBED S-A
NON-MAGNETIC SEPARATE
5100 oE

FIG. 8

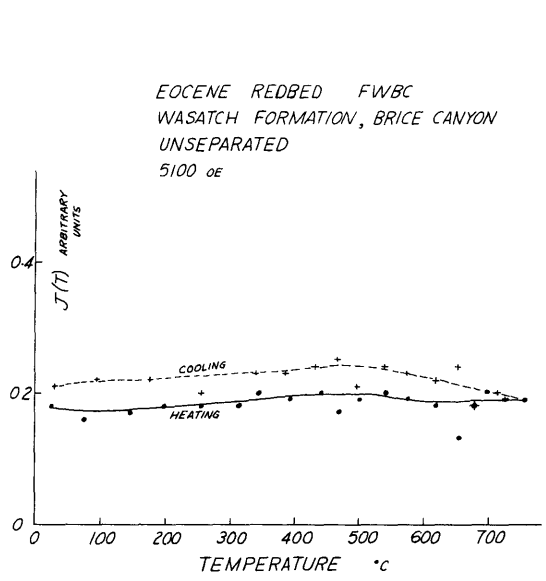
EOCENE REDBED FWBC
WASATCH FORMATION, BRICE CANYON
UNSEPARATED
5100 oE
J(T) ARBITRARY UNITS
0.4
0.2
0
COOLING
HEATING
0
100
200
300
400
500
600
700
TEMPERATURE °C

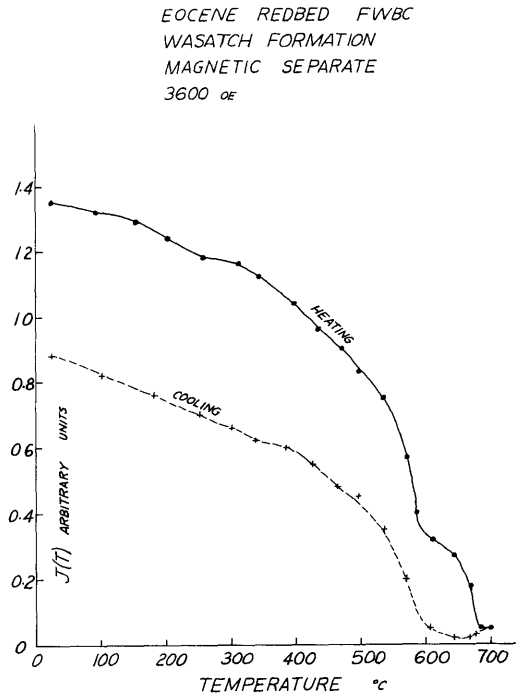
EOCENE REDBED FWBC
WASATCH FORMATION
MAGNETIC SEPARATE
3600 oE
1.4
1.2
1.0
0.8
0.6
0.4
0.2
0
J(T) ARBITRARY UNITS
HEATING
COOLING
0
100
200
300
400
500
600
700
TEMPERATURE °C

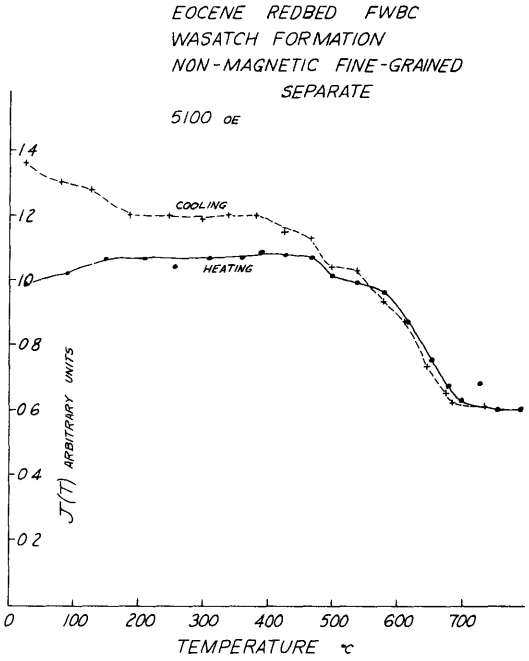
EOCENE REDBED FWBC
WASATCH FORMATION
NON-MAGNETIC FINE-GRAINED
SEPARATE
5100 oE
1.4
1.2
1.0
0.8
0.6
0.4
0.2
J(T) ARBITRARY UNITS
COOLING
HEATING
0
100
200
300
400
500
600
700
TEMPERATURE °C

absence of paramagnetic material, suggests that this formation might have come from a reworking and redeposition of an older sediment.

Results 6. Permian and Pennsylvanian Red Sandstones

Samples of well-consolidated ancient red sandstones from Colorado, Permian and Pennsylvanian in age, were analysed thermomagnetically to allow a comparison with the results for younger rocks, as outlined in previous sections. According to the character of their natural remanent magnetization as measured with a spinner magnetometer, McMahon (1966) has divided the Permian samples into two groups: those in the Lykins and Fountain formations, which were stable and easy to measure, and those in the Lyons and Ingleside formations, which were neither. The intensity of magnetization of the stable samples was 10^{-6} - 10^{-5} emu/cm^3, greater than that of the Pliocene arkoses described in section 4.

In general, the separation process yielded much less magnetic material from the Permian rocks than from the Pliocene ones. Also, what there was of it seemed to be less strongly magnetized, to judge from the rather sluggish action

under the hand magnet and from the larger field gradients required to cause suitable deflections in the magnetic balance. Features of the thermomagnetic curves give an explanation for this behavior, as discussed below.

To consider first the Lykins and Fountain red beds, which had stable, measurable magnetization, Figure 9 shows the results for a sample from the Fountain formation. The non-magnetic separate shows weak but fairly well-defined paramagnetic material and some hematite, while the magnetic separate presents dominant magnetite, little maghemite breakdown, and a surprisingly large hematite magnetization above the magnetite Curie point. These features, small maghemite content and good ferromagnesian silicate indication, seemed common to this group of samples.

The strong hematite showing in the magnetic separate suggests a reason for the relatively weak total magnetization of the particles in this separate. If the hematite in the particles was a result of incomplete alteration of original magnetite, there might still be sufficient magnetite remaining inside the hematite haloes for the particles to be

FIG. 9

PERMIAN REDBED DP250·2E
FOUNTAIN FORMATION
MAGNETIC SEPARATE
1300 oE

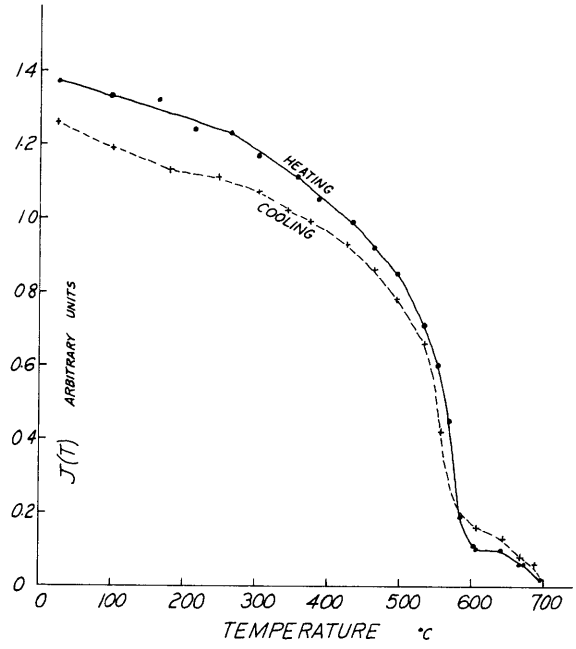

PERMIAN REDBED DP250·2E
FOUNTAIN FORMATION
NON-MAGNETIC SEPARATE
5100 oE.

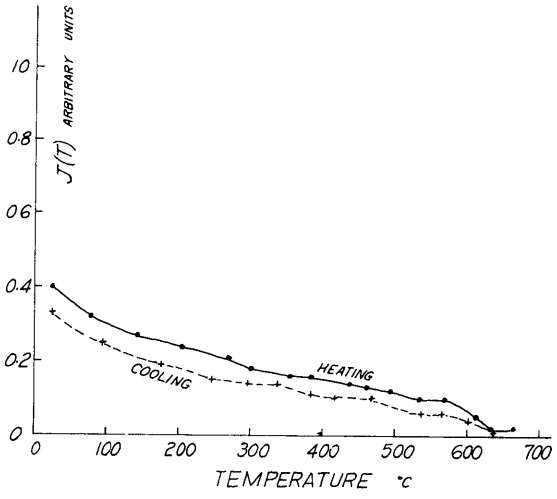

attracted to the hand magnet and to give the material a magnetite Curie point (580°C) under thermomagnetic analysis.

Turning to the Lyons and Ingleside red beds, which gave poor results on spinning, the curves for a sample from the Lyons formation are drawn in Figure 10. The fairly large maghemite downshift on the magnetic separate (see Table III) and the notable absence of a paramagnetic shape to the curve for the non-magnetic separate seem typical of this group. Another sample from the Lyons formation, taken at depth in a drill core to obtain a specimen unaffected by recent near-surface weathering, contains more maghemite (see Table III) and also appreciable magnetite (a Curie point at 590°C on the magnetic-separate curve in Figure 27). The 750°C Curie point suggests iron contamination from the drill pipe.

Five observations from the magnetic separates of these two samples — abundance of hematite, absence of magnetite and lesser maghemite content in the surface sample; greater maghemite breakdown and presence of magnetite in the subsurface sample — indicate that the iron oxides in the surface sample have been oxidized more than those in the subsurface sample.

FIG. 10

PERMIAN REDBED 6M 282.5-2
LYONS FORMATION
UNSEPARATED
5100 oE

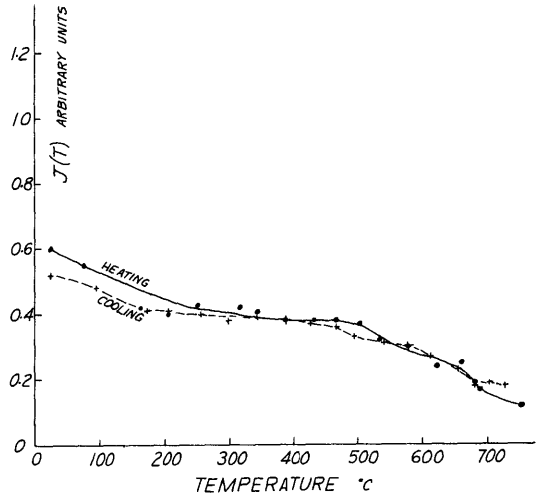

PERMIAN REDBED 6M 282.5-2
MAGNETIC SEPARATE
2500 oE

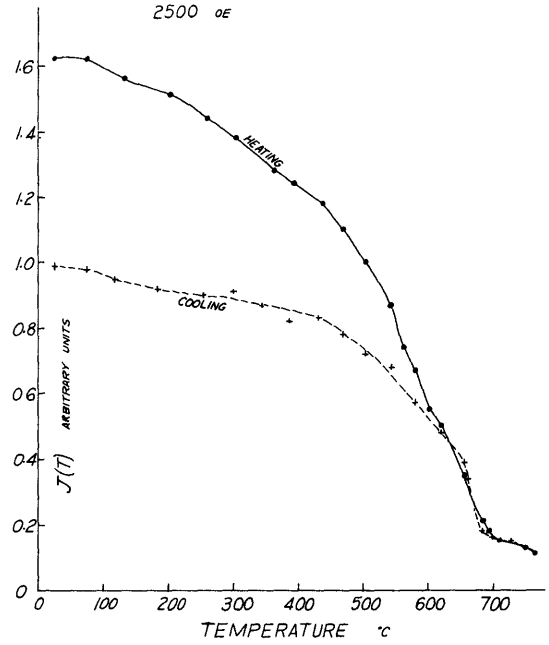

PERMIAN REDBED 6M 282.5-2
FINE-GRAINED NON-MAGNETIC
SEPARATE
5100 oE.

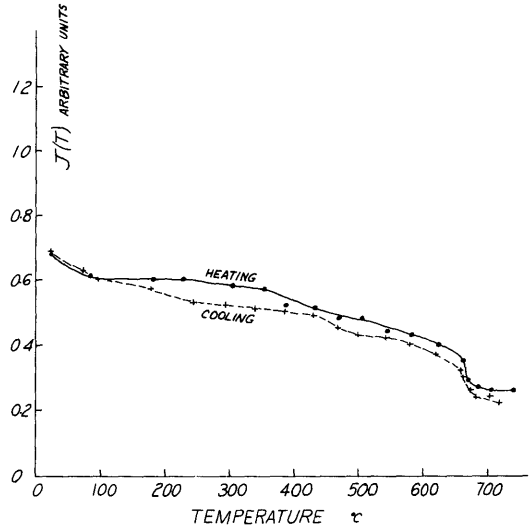

PERMIAN REDBED 6M 282.5-2
COARSE-GRAINED NON-MAGNETIC
SEPARATE
5100 oE

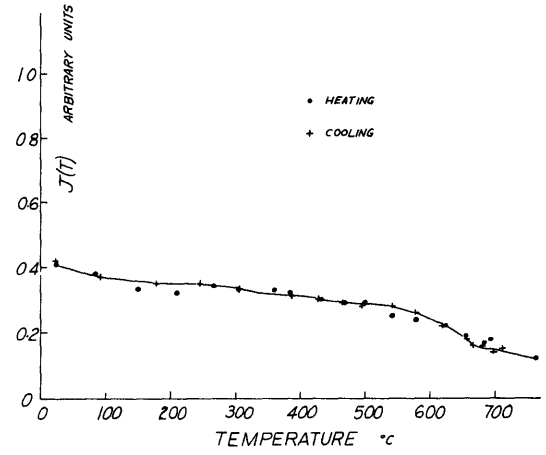

TABLE III

Decrease in room-temperature magnetization of Permian and Pennsylvanian red sandstones after heating as a percentage of initial magnetization

Sample	Whole rock	Magnetic separate (maghemite breakdown)	Non-magnetic separate
Lykins 6M LK770 IE	38	36	6
LHR LK3		49	9
Lyons 6M 282.5-2 (surface)	13	39	-1*
RMA 9891 (subsurface)		56	
Ingleside DP E-2-0		64	
Fountain DP 250-2E		8	18
FF 75-1		1	
Minturn RSC 880.2		59	24

*magnetization increased after heating

McMahon (personal communication to D.W. Strangway) described the subsurface sample as having "even staining, as though it had not been materially affected by circulating ground waters such as seem to have been acting on surface outcrops...". Perhaps the oxygen carried in the ground waters has had a considerable effect on the magnetic minerals in the surface and near-surface rocks of this formation.

McMahon (1966) has observed that samples containing micaceous material and fine-grained magnetite tend to give the most reliable paleomagnetic data. The curves presented here seem to confirm these observations of the mineral content of the stable and unstable rocks, but statistically this cannot be a rigorous conclusion because of the limited number of samples considered.

Results 7. Thermal Breakdown of Lepidocrocite

To develop a feeling for the identification of lepidocrocite (γFeOOH, or FeO(OH)) under thermomagnetic analysis, a sample of well-formed flake crystals of the material was seen, yielding the results shown in Figure 11. The very startling increase in saturation magnetization beginning at

FIG. 11 -50-

THERMOMAGNETIC CURVE FOR LEPIDOCROCITE

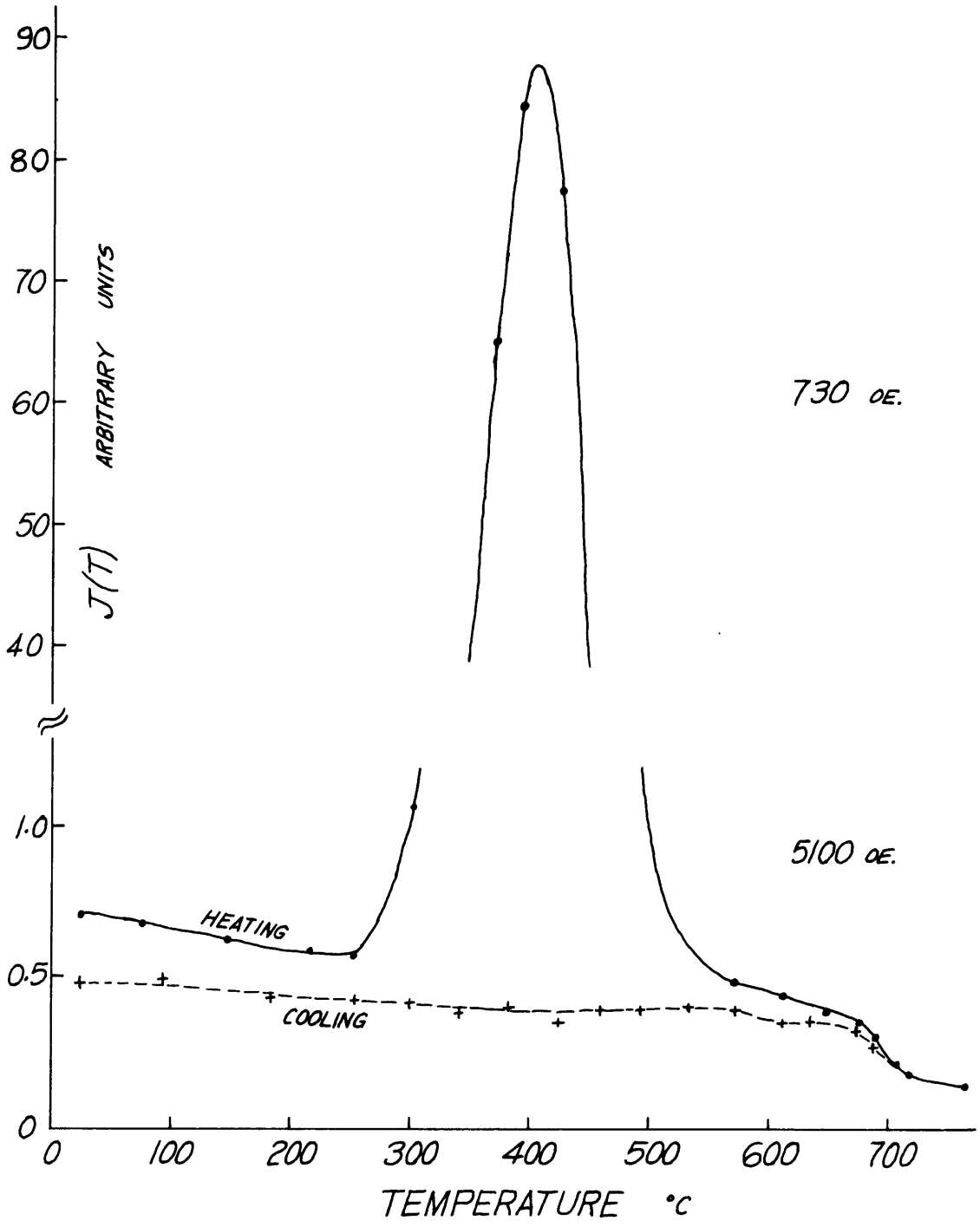

260°C followed by an equally sharp decrease during further heating through the range 400° - 500°C suggests this sequence:

$$\text{lepidocrocite} \xrightarrow[260°\text{-}400°\text{C}]{} \text{maghemite} \xrightarrow[400°\text{-}500°\text{C}]{} \text{hematite}$$

This reaction chain has been proposed by Michel and Gallissot (1937) from thermomagnetic analyses similar to this, and by Kulp and Trites (1951) from differential thermal analysis, Kelley (1956) reports that goethite (α FeOOH, or, more correctly, $HFeO_2$) in poorly-formed crystals may also decompose by way of maghemite to hematite, in contrast to its behavior in well-formed crystals, when it transforms directly to hematite at about 400°C.

A rough calculation, substituting typical values for the parameters in equation (A.7) in Appendix A, shows that an increase in a sample's maghemite content of 1 part by weight in 10^3 or 10^4 should be readily identifiable on the thermomagnetic curves, owing to the large increase in saturation magnetization. This would then suggest that the sensitivity of the magnetic balance in detecting lepidocrocite

or poorly-crystallized goethite is of the order of 1 part by weight in 10^3 or 10^4, assuming that these oxyhydroxides do break down to maghemite as outlined.

A scan of the curves for non-magnetic separates, where such an effect would most likely be noted because of the high magnetic field gradients generally applied, gives no positive results. It may then be concluded that the content of lepidocrocite and poorly-crystallized goethite in the samples examined is less than 1 part by weight in 10^3 or 10^4.

It may well be, however, that at some time in the past these oxyhydroxides of iron were considerably more abundant in the rocks sampled than they are now, but that they have since dehydrated to iron oxides with consequent changes in magnetic properties. If lepidocrocite had formed during the oxidation of the iron in biotites while the sediment was at the surface, and then decomposed soon after deposition (Creer 1962) or during the later burial and heating of the sediment, highly magnetic maghemite might have appeared. Chamalaun (1964) notes that the Old Lower Red Sandstones of Britain, if buried to a depth of 9 km, could have reached

a temperature of 200°C; with sufficient time at this temperature, the lepidocrocite→ maghemite reaction might have taken place. It is not known how this new magnetic material would be aligned with respect to the ambient geomagnetic field; if it were coherent with the field, the direction of the total magnetization of the rock could be appreciably changed. Thus iron oxyhydroxides could be important in the magnetizing of a red sediment.

IV. CONCLUSIONS AND SUGGESTIONS FOR FURTHER WORK

In conclusion, the results of this work can be presented as follows:

1. The young Pliocene arkoses contain abundant magnetite, an intermediate quantity of maghemite which appears to increase with age, and a certain amount of hematite. The content of unweathered ferromagnesian minerals, especially biotite, is high; biotite seems to be breaking down to ferrimagnetic material.

2. Pliocene muds, contemporary with the arkoses, have considerably more maghemite and less magnetite than the arkoses. This probably reflects differences in the source rocks and in the modes of transportation and deposition of the sediments; the muds were laid down in a river delta, whereas the arkoses were carried and deposited in the violent flash floods of a desert environment.

3. The ancient red sandstones of Permian and Pennsylvanian age generally have less magnetite and more maghemite than the young Pliocene arkoses, magnetite having been oxidized to maghemite and hematite in the older rocks.

There seems to be some correlation between paramagnetic mica content and stability of natural remanent magnetism; perhaps these minerals act as a buffer against chemical attack on the minerals which carry the coherent magnetization, or perhaps they act as a host in which fine-grained stable hematite can form to give the sediment a coherent magnetization.

Such a formation from biotite of magnetic material in amounts which hardly show on the J_s - T curves could have important effects on the natural remanent magnetization (NRM) of the red sediments. Irving (1964, p. 97) writes that "it seems clear that the carrier of NRM is only a small fraction of the total magnetic material present", so the creation of small quantities of fine-grained stable magnetic minerals aligned in the ambient geomagnetic field could give the rock a net magnetization if it previously lacked one. Alternatively, the addition of new material aligned in a geomagnetic field which had changed direction since the original magnetization was acquired would yield a resultant magnetization with an intermediate orientation.

4. Lepidocrocite and poorly-crystallized goethite are at present relatively unimportant as iron-bearing minerals in these sediments, amounting to less than 1 part by weight in 10^3 to 10^4. It is noted that their formation and subsequent breakdown to iron oxides at some time in the past could have had a considerable effect on the natural remanent magnetization of the red beds.

Three suggestions could be made for future work with these red sediments. One is connected with the collection of the samples, the other two with laboratory experiments. It is suspected that, owing to the inhomogeneity of the arkoses, as much variation in magnetic properties would be found along a given horizon as across a number of them. Sampling horizontally as well as vertically would be an obvious way to investigate this problem.

To gather further data on the size distribution of iron oxide mineral grains, magnetization-temperature measurements at cryogenic temperatures might be used to trace the growth of particles still small enough to behave superparamagnetically. This method has been used elsewhere; see Creer (1961).

Thermal demagnetization of those samples with stable natural remanent magnetization might indicate which of the iron oxide minerals carries this magnetization. Comparison of the demagnetization curves with the saturation magnetization curves presented here could show whether the remanence is due to one or more of the detritally-aligned minerals previously magnetized on cooling through its Curie point, or whether blocking temperature phenomena are involved; see Chamalaun (1964). This technique would be more applicable to the ancient red beds than to the young arkoses; the magnetization of the latter is already so weak that even partial removal might make further measurements impossible.

References

Akimoto, S., 1954: "Thermomagnetic studies of ferromagnetic minerals contained in igneous rocks", J. Geomag. Geoelec. 6, 1-14.

Bates, L.F., 1951: Modern Magnetism (3d edition). Cambridge University Press, Cambridge. 506 pp.

Buddington, A.F., and D.H. Lindsley, 1964: "Iron-titanium oxide minerals and synthetic equivalents", J. Petrol. 5, 275-309.

Chamalaun, F.H., 1964: "Origin of the secondary magnetization of the Old Red Sandstones of the Anglo-Welsh Cuvette", J. Geophys. Res. 69, 4327-4337.

Chaudron, G., and A. Michel, 1938: "Charactères thermomagnétiques du sesquioxyde de fer cubique", C.R. Acad. Sci. Paris 208, 90-92.

Collinson, D.W., 1965a: "The remanent magnetization and magnetic properties of red sediments", Geophys. J. 10, 105-126.

Collinson, D.W., 1965b: "Origin of remanent magnetization and initial susceptibility of certain red sandstones", Geophys. J. 9, 203-217.

Collinson, D.W., 1965c: "Depositional remanent magnetization in sediments", J. Geophys. Res. 70, 4663-4668.

Collinson, D.W., 1966: "Carrier of remanent magnetization in certain red sandstones", Nature 210, 516-517.

Creer, K.M., 1961: "Superparamagnetism in red sandstones", Geophys. J. 5, 16-28.

Creer, K.M., 1962: "On the origin of the magnetization of red beds", J. Geomag. Geoelec. 13, 86-100.

Helsley, C.E., 1964: "Evidence of post-depositional magnetization of certain red sediments", Trans. A.G.U. 45, 38.

Irving, E., 1964: Paleomagnetism and its application to geological and geophysical problems. John Wiley & Sons, Inc., New York. 399 pp.

Kelley, W.C., 1956: "Application of differential thermal analysis to identification of the natural hydrous ferric oxides", Am. Mineral. 41, 353-355.

King, R.F., and A.J. Rees, 1966: "Detrital magnetism in sediments: an examination of some theoretical models", J. Geophys. Res. 71, 561-571.

Kobayashi, K., 1962: "Magnetization-blocking process by volume development of ferromagnetic fine particles", J. Phys. Soc. Japan 17, suppl. BI, 695-698.

Kulp, J.L., and A.F. Trites, 1951: "Differential thermal analysis of natural hydrous ferric oxides", Am. Mineral. 36, 23-44.

Kyrnine, P.D., 1950: "Petrology, stratigraphy, and origin of the Triassic sedimentary rocks of Connecticut", Bull. Conn. Geol. Nat. Hist. Surv. 73.

McMahon, B., 1966: Ph.D. thesis, Department of Geology, University of Colorado.

Michel, A., and M. Gallissot, 1938: "Relation entre l'état de crystallisation et l'amplitude de l'anomalie thermo-magnétique de la lépidocrocite", C.R. Acad. Sci. Paris 206, 1252-1254.

Nagata, T., 1961: Rock magnetism (2d edition). Maruzen Press, Tokyo. 350 pp.

Néel, L., 1949: "Theorie du traînage magnétique des ferro-magnétiques en grains fins avec application aux terres cuites", Ann. Geophys. 5, 99.

Néel, L., 1955: "Some theoretical aspects of rock magnetism", Phil. Mag. Supp. Adv. Phys. 4, 191-243.

Nicholls, G.D., 1955: "The mineralogy of rock magnetism", Phil. Mag. Supp. Adv. Phys. 4, 113-190.

Opdyke, N.D., 1961: "The paleomagnetism of the New Jersey Triassic: a field study of inclination error in red sediments", J. Geophys. Res. 66, 1941-1949.

Pouillard, E., 1950: "Sur le comportement de l'alumine et de l'oxyde de titane vis-à-vis des oxydes de fer", Ann. Chimie 5, 164.

Strangway, D.W., 1958: "Measurement of the thermal variation of the susceptibility of rocks", M.A. thesis, University of Toronto.

Ising, G., 1943: "On the magnetic properties of varved clay", Arkiv Mat. Astron. Fysik A 29, 1-37.

APPENDIX A

The Quartz-Spring Magnetic Balance

Theory of operation

To investigate the thermal variation of the susceptibility of the paramagnetic minerals and of the saturation magnetization of the ferrimagnetic minerals in the red beds, a translational balance patterned after that of Akimoto (1954) was built, using the extension of a fused quartz spring to measure the force on magnetic material in a non-uniform magnetic field. The potential energy of magnetic material with volume v in a magnetic field H is given by

$$\phi_1 = -\frac{\mu H^2}{8\pi} V \qquad \text{(A.1)}$$

The material displaces a volume v of the surrounding air which had a potential energy

$$\phi_2 = -\frac{H^2}{8\pi} V \qquad (\mu_{AIR} \approx 1) \qquad \text{(A.2)}$$

with a resulting change in potential given by

$$\phi_1 - \phi_2 = -\frac{(\mu-1)H^2}{8\pi} V \tag{A.3}$$

and the force on the sample is the negative gradient of this change in potential

$$\vec{F} = -\nabla\left[\frac{(\mu-1)}{8\pi} H^2 V\right] = \frac{(\mu-1)V}{8\pi} \nabla H^2 \tag{A.4}$$

If one component of ∇H^2 is much greater than the other two,

$$F_z = \frac{(\mu-1)}{4\pi} V \; H \; \frac{dH}{dz} \tag{A.5}$$

Taking $\mu = 1 + 4\pi\chi(T)$, where $\chi(T)$ is a volume susceptibility, a function of the absolute temperature T, this becomes, for a paramagnetic substance,

$$F_z = V \chi(T) H \frac{dH}{dz} \tag{A.6}$$

and generalizing for a ferrimagnetic substance with volume saturation magnetization $J_s(T)$,

$$F_z = v J_s(T) \frac{dH}{dz} \qquad (A.7)$$

See Bates (1951, p. 111, 122).

Construction Details (see Figure 12)

The quartz coil spring used in most of the work was supplied by the Nakamura Seisakusho Company of Tokyo, Japan. It had 130 turns, each 10 mm in diameter, a maximum load of 0.3 gm, and a spring constant at room temperature of approximately 15 mg/cm.

A quartz glass tube, 22 mm i.d., supported the quartz spring and provided a form around which the sample-heating furnace was wound. The tube was closed off at the bottom and capped at the top through a ground-glass ball joint, allowing evacuation to a pressure less than 10 microns Hg in those cases where it was desired to inhibit oxidation of the sample. However, most samples were heated in air at atmospheric pressure.

For the furnace, 34 double turns of 22 B & S gauge non-magnetic chromel wire, about 1 ohm/ft, were wound non-

FIG. 12
QUARTZ - SPRING
MAGNETIC BALANCE

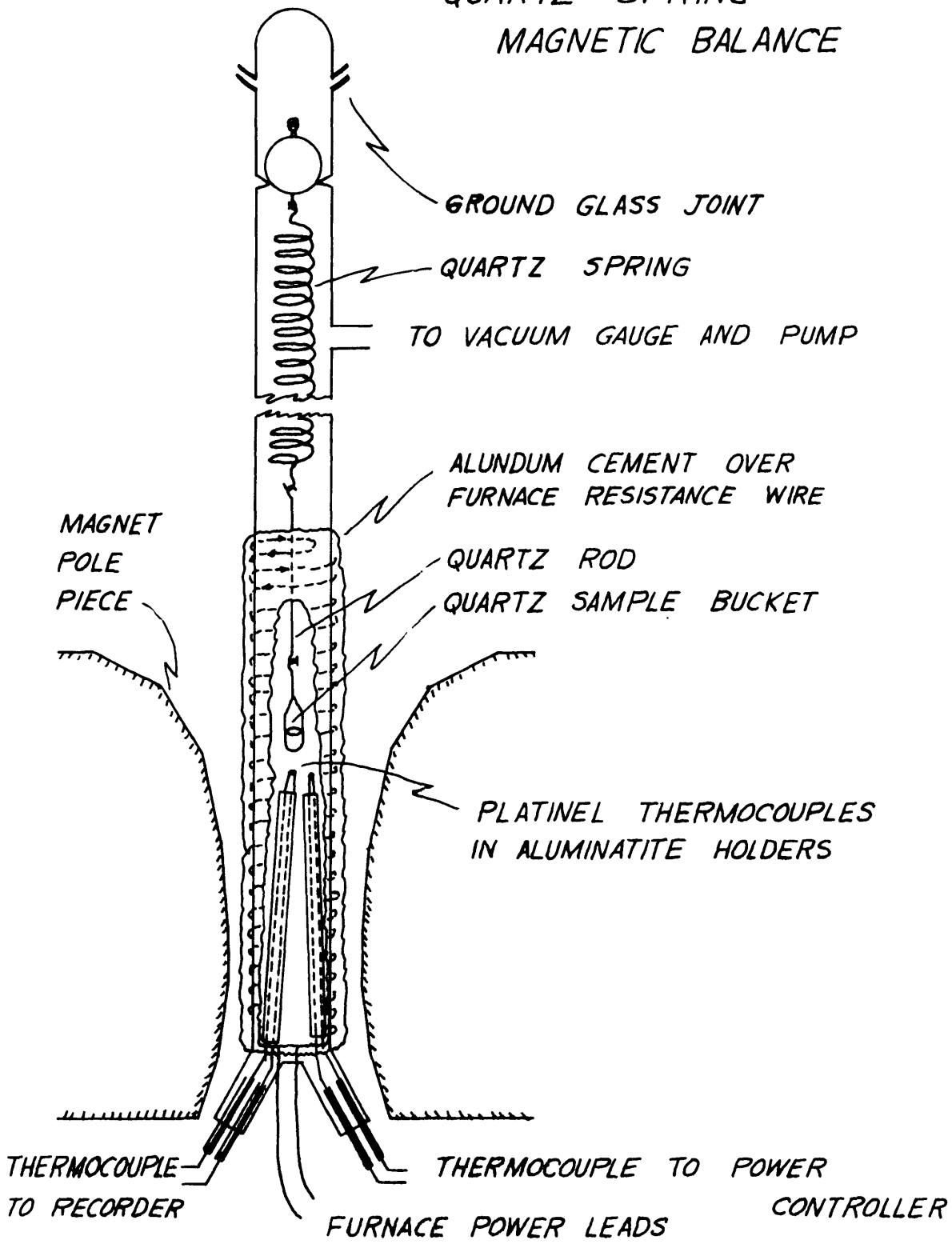

inductively over asbestos paper around the glass tube, then covered with alundum paste for support and insulation. The paste was applied as a wet slurry; when it had dried, heating to 750°C fired the material in place. Further insulation, asbestos paper and aluminum foil, gave the furnace better temperature stability and protected the pole pieces of the electromagnet.

Two thermocouples occupied the lower half of the furnace. These had platinel II-type elements from Engelhard Industries of New Jersey, chosen for their non-magnetic noble-metal composition and for their relatively high output millivoltage, close to that of the magnetic (Strangway 1958) type K chromel-alumel thermocouples. The platinel thermocouples were silver-soldered into Kovar low-thermal-expansion metal tubes which were sealed into the glass tube. The output of one of the thermocouples went to a Y-t recorder, to measure and record the furnace temperature; the other formed the feedback element for the temperature-power control system.

Control of the furnace temperature was attempted through a programmable temperature-power unit with proportional control

and rate-reset action, from Research Incorporated of Minnesota. The temperature was changed linearly with time in increments of about 40 C° and allowed to stabilize at each step before a reading was taken. A complete cycle, heating from room temperature to 750°C and then cooling, required about two-and-a-half hours' time. Some problems were encountered due to the changing response of the furnace with temperature; radiation heat loss, proportional to the fourth power of the absolute temperature, was high enough in the upper-temperature range to cause system instabilities. In the lower ranges overall losses were so small that severe temperature overshoot sometimes complicated the operation.

The inhomogeneous magnetic field required in the experiment was produced by an electromagnet from Spectromagnetic Industries of California. Specially-cut pole pieces gave a field in which H dH/dz was constant for variation of the sample location in the z direction; Figure 13 shows the variation of the field in the magnet gap. This was ideal for the paramagnetic minerals (see equation (A.6)). Working with the ferrimagnetic minerals required a field large

FIG. 13

SPATIAL VARIATION OF ELECTROMAGNET FIELD

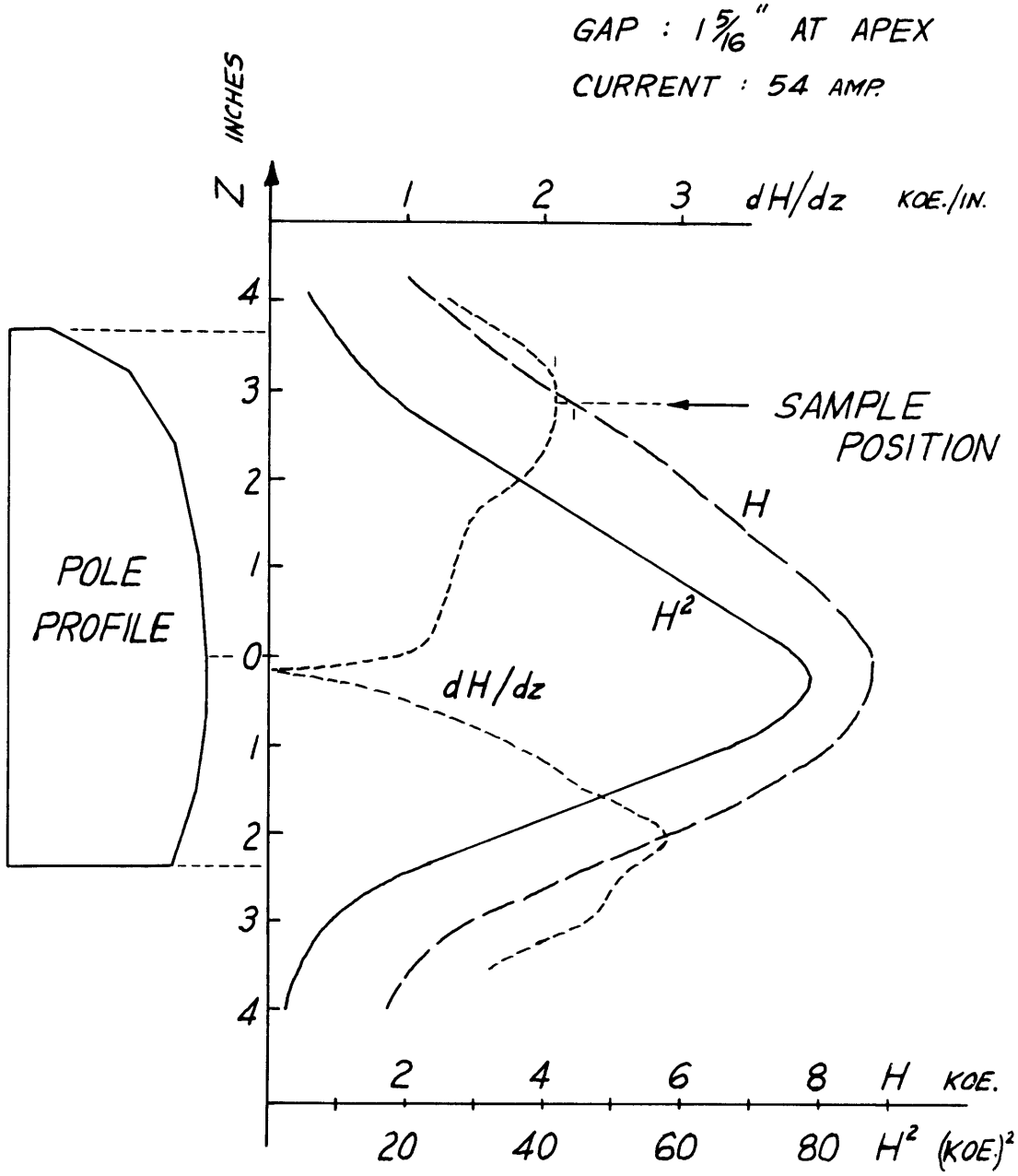

enough to produce saturation and a field with dH/dz constant (equation (A.7)); the latter condition was met by positioning the sample at a broad maximum of dH/dz, where the magnitude of the force would be least affected by movement of the sample in the direction of the force (Nagata 1961, p. 47).

The deflection of the spring was observed with a Gaertner telemicroscope fitted with a scale eyepiece micrometer. To allow for the thermal change of the spring's elastic constant (about one percent per 100 C°) readings were made first with the field off and then with the field applied; the difference between these readings was plotted against temperature to give the J_s - T relationship.

Temperature Calibration

The apparatus thermocouple was compared with another thermocouple from Engelhard Industries which had specified tolerances on its output throughout the temperature range. Then, as a check, curves were run for substances with known Curie temperatures, such as magnetite and hematite, 99.999% pure nickel, and a volcanic rock measured by Larson on equipment at the University of Tokyo. Some of these curves are shown in Figure 14.

FIG. 14

CALIBRATION OF MAGNETIC BALANCE

USING SUBSTANCES WITH KNOWN CURIE TEMPERATURES

NICKEL	358 °C
MAGNETITE	578 °C
HEMATITE	680 °C

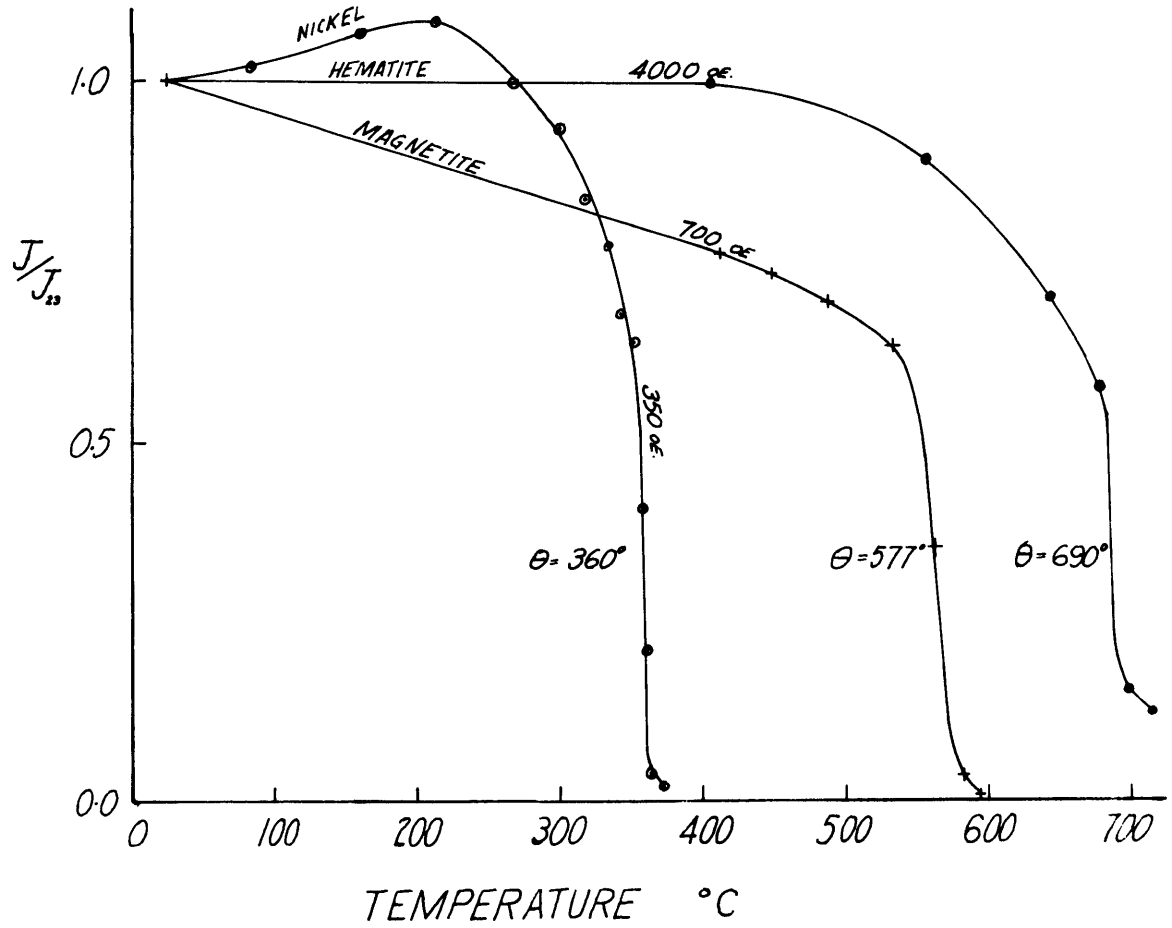

APPENDIX B

Thermomagnetic Curves

Experimental curves are presented as follows:

Figure No.	Sample		Page
	Pleistocene soils		
2	Hermosillo	SP4	27
2	San Diego	MCS-1	27
	Pleistocene mud		
3	San Felipe	E.B.	29
	Pliocene muds		
15	San Felipe	1A	72
16		SF 34	73
	Pliocene red beds		
17	Baja California	PE 13	74
18		PE 70	75
6		PE 182	37
19		PE 270	76
20		PE 408	77
21		PE 452	78
22		PE 523	79
23		PC 27	80
24		WF-RB-4	81
	Oligocene red bed		
7	Sespe	S-A	41
8	Eocene red bed		
	Wasatch	FWBC	42

Figure No.	Sample		Page
	Permian red beds		
25	Lykins	6M 770-1E	82
26		LHR LK3	83
10	Lyons	6M 282.5-2	47
27		RMA 9891	84
28	Ingleside	DP E-2-0	85
9	Fountain	DP 250-2E	45
29		FF 75-1	86
	Pennsylvanian red bed		
30	Minturn	RSC 880.2	87

FIG. 15

PLIOCENE MUD 1A (SAN FELIPE)
UNSEPARATED
5100 oe.

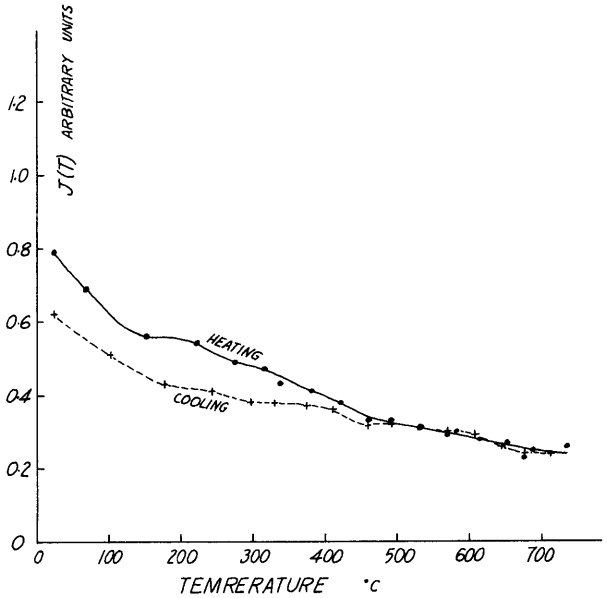

PLIOCENE MUD 1A
MAGNETIC SEPARATE
385 oe.

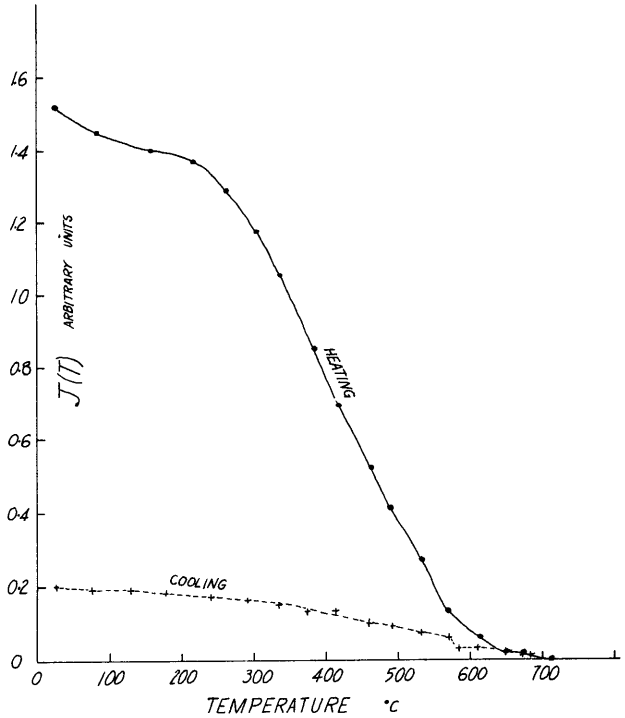

FIG. 16

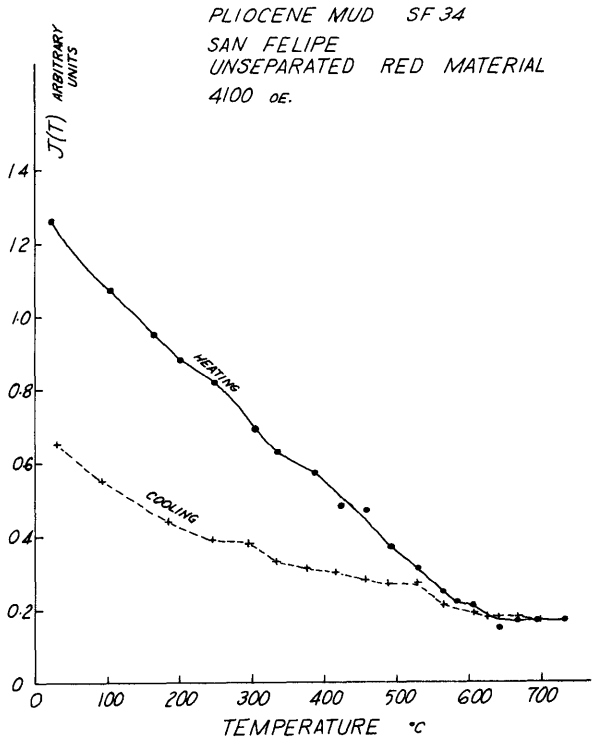
PLIOCENE MUD SF 34
SAN FELIPE
UNSEPARATED RED MATERIAL
4100 oE.
J(T) ARBITRARY UNITS
1.4
1.2
1.0
0.8
0.6
0.4
0.2
0
HEATING
COOLING
0
100
200
300
400
500
600
700
TEMPERATURE °C

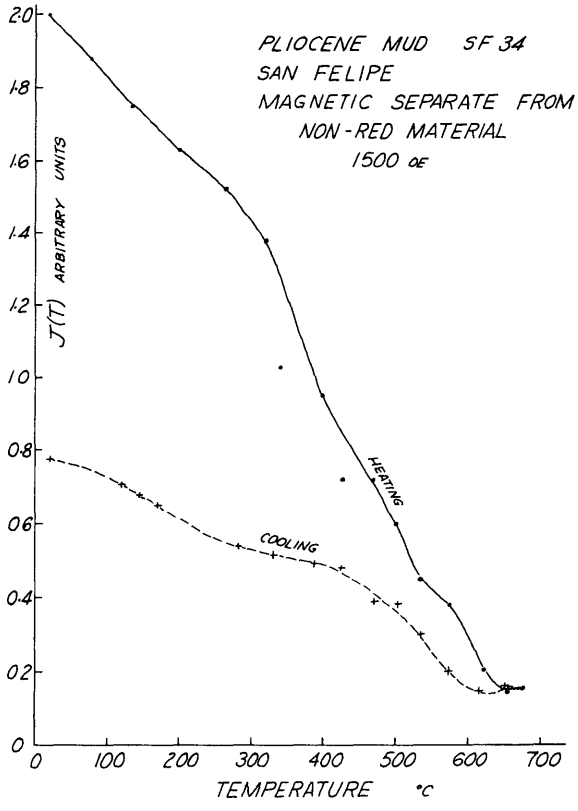
PLIOCENE MUD SF 34
SAN FELIPE
MAGNETIC SEPARATE FROM
NON-RED MATERIAL
1500 oE
J(T) ARBITRARY UNITS
2.0
1.8
1.6
1.4
1.2
1.0
0.8
0.6
0.4
0.2
0
HEATING
COOLING
0
100
200
300
400
500
600
700
TEMPERATURE °C

FIG. 17

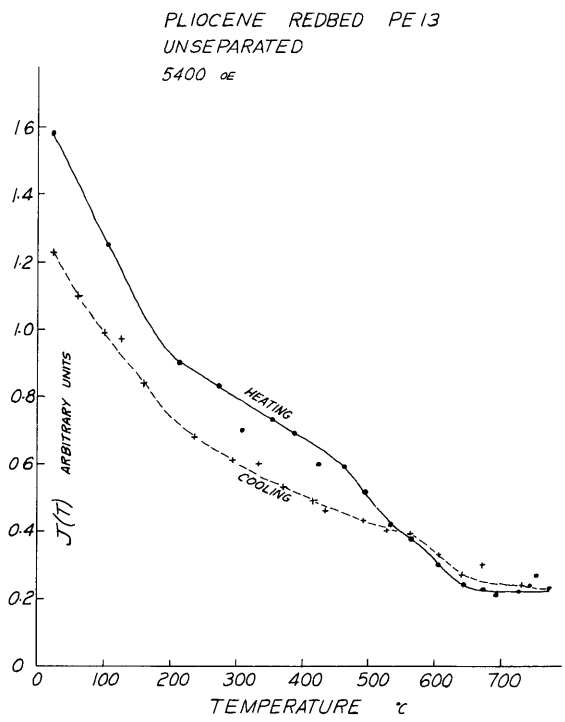
PLIOCENE REDBED PE 13
UNSEPARATED
5400 oE
J(T) ARBITRARY UNITS
HEATING
COOLING
TEMPERATURE °C

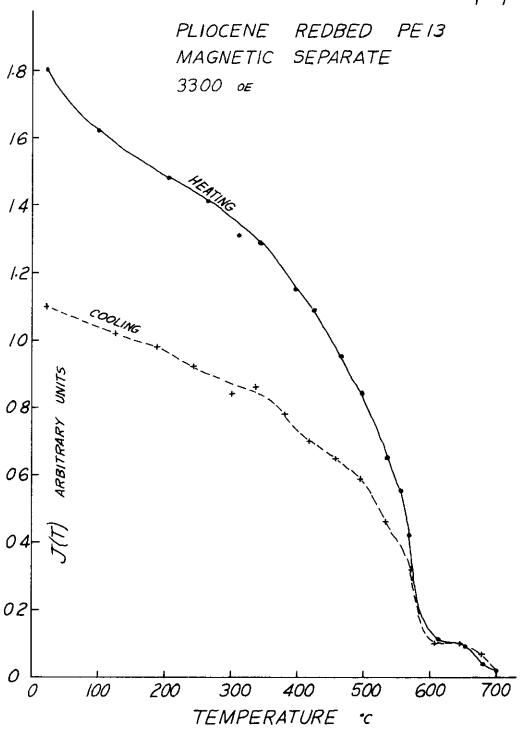
PLIOCENE REDBED PE 13
MAGNETIC SEPARATE
3300 oE
J(T) ARBITRARY UNITS
HEATING
COOLING
TEMPERATURE °C

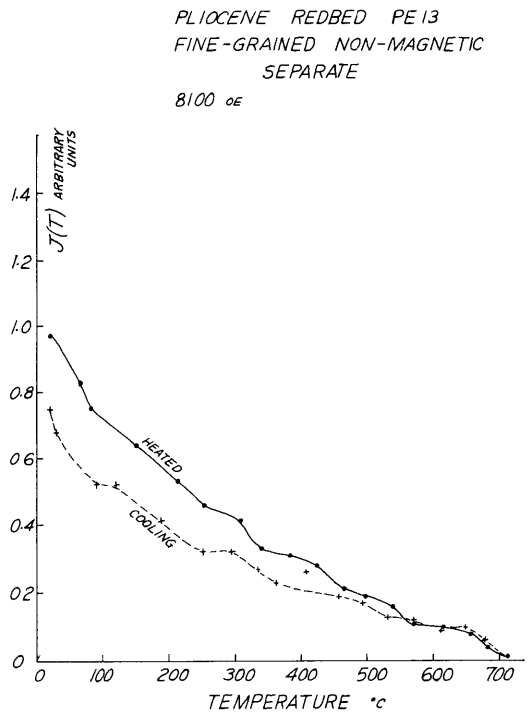
PLIOCENE REDBED PE 13
FINE-GRAINED NON-MAGNETIC
SEPARATE
8100 oE
J(T) ARBITRARY UNITS
HEATED
COOLING
TEMPERATURE °C

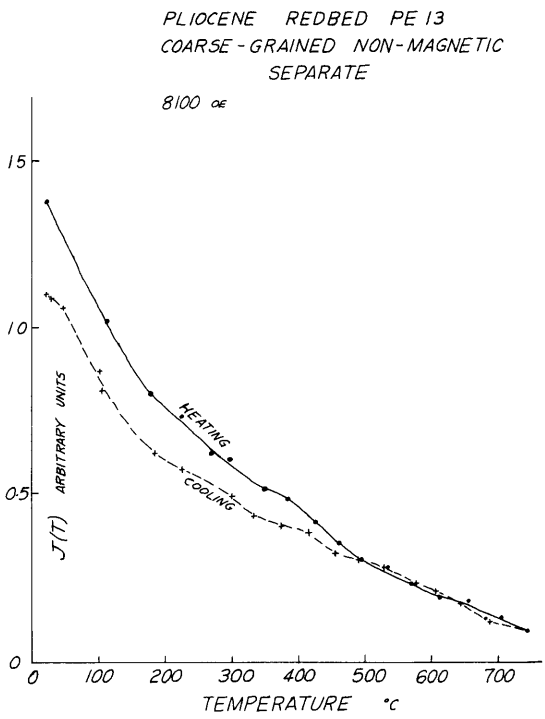
PLIOCENE REDBED PE 13
COARSE-GRAINED NON-MAGNETIC
SEPARATE
8100 oE
J(T) ARBITRARY UNITS
HEATING
COOLING
TEMPERATURE °C

FIG. 18

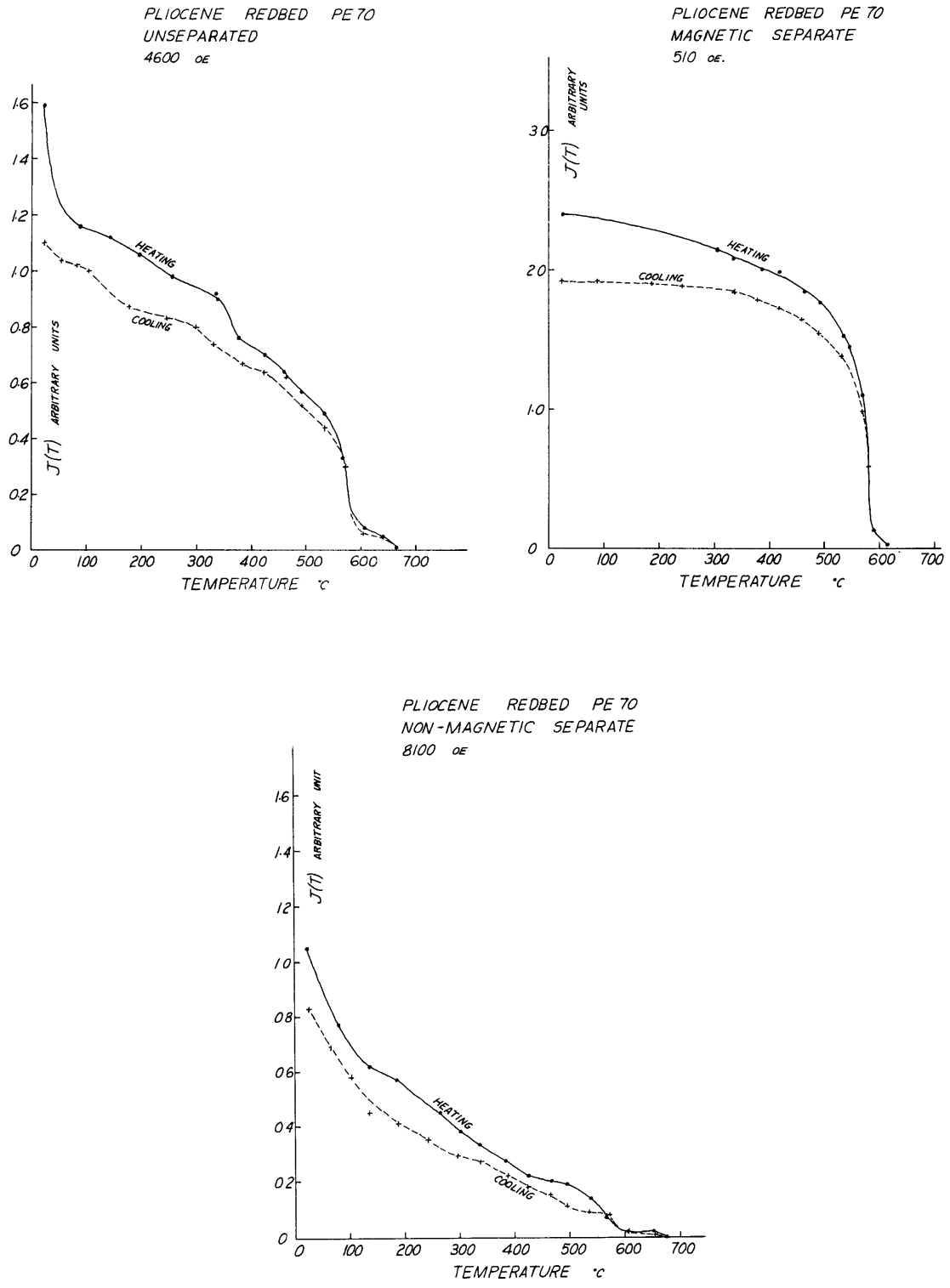
PLIOCENE REDBED PE 70
UNSEPARATED
4600 oE
J(T) ARBITRARY UNITS
HEATING
COOLING
TEMPERATURE °C
PLIOCENE REDBED PE 70
MAGNETIC SEPARATE
510 oE.
J(T) ARBITRARY UNITS
HEATING
COOLING
TEMPERATURE °C
PLIOCENE REDBED PE 70
NON-MAGNETIC SEPARATE
8100 oE
J(T) ARBITRARY UNIT
HEATING
COOLING
TEMPERATURE °C

FIG. 19

PLIOCENE REDBED PE 270
UNSEPARATED
4270 oE

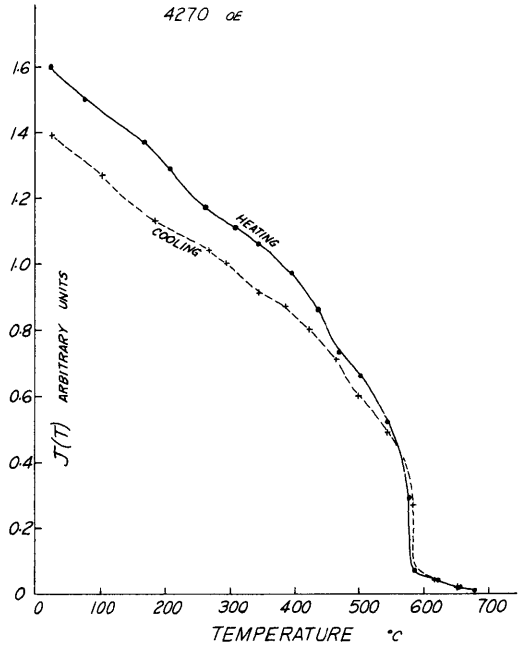

PLIOCENE REDBED PE 270
MAGNETIC SEPARATE
1125 oE

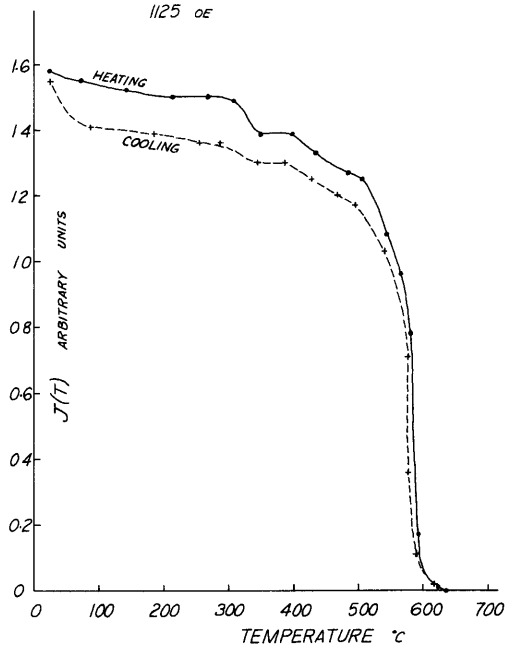

PLIOCENE REDBED PE 270
NON-MAGNETIC SEPARATE
5100 oE.

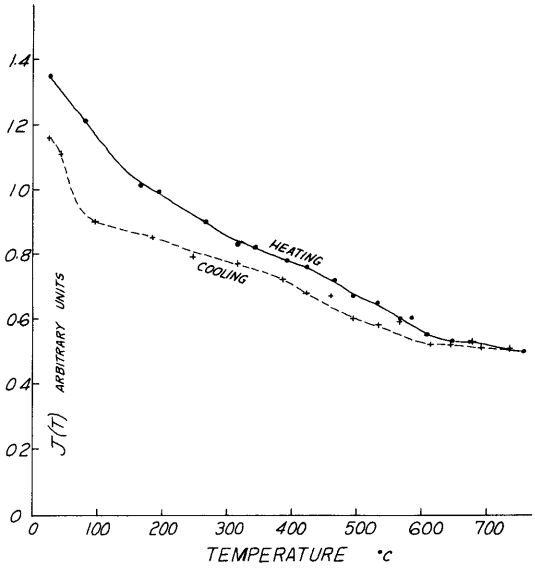

FIG. 20

PLIOCENE REDBED PE 408
RED MATERIAL SCRAPED FROM
SAMPLE
1900 oE

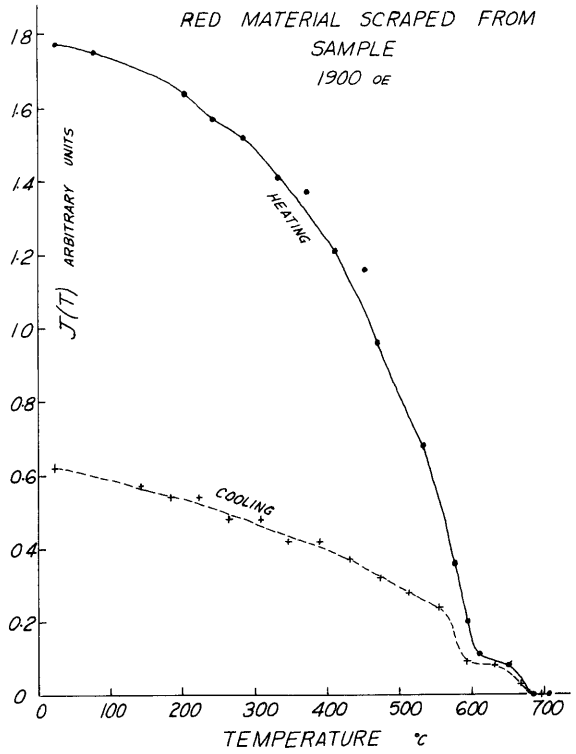

PLIOCENE REDBED PE 408
MAGNETIC SEPARATE
660 oE

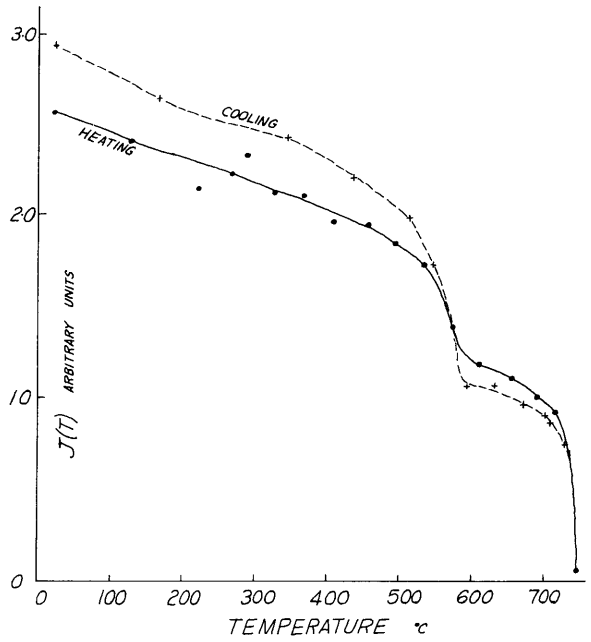

FIG. 21

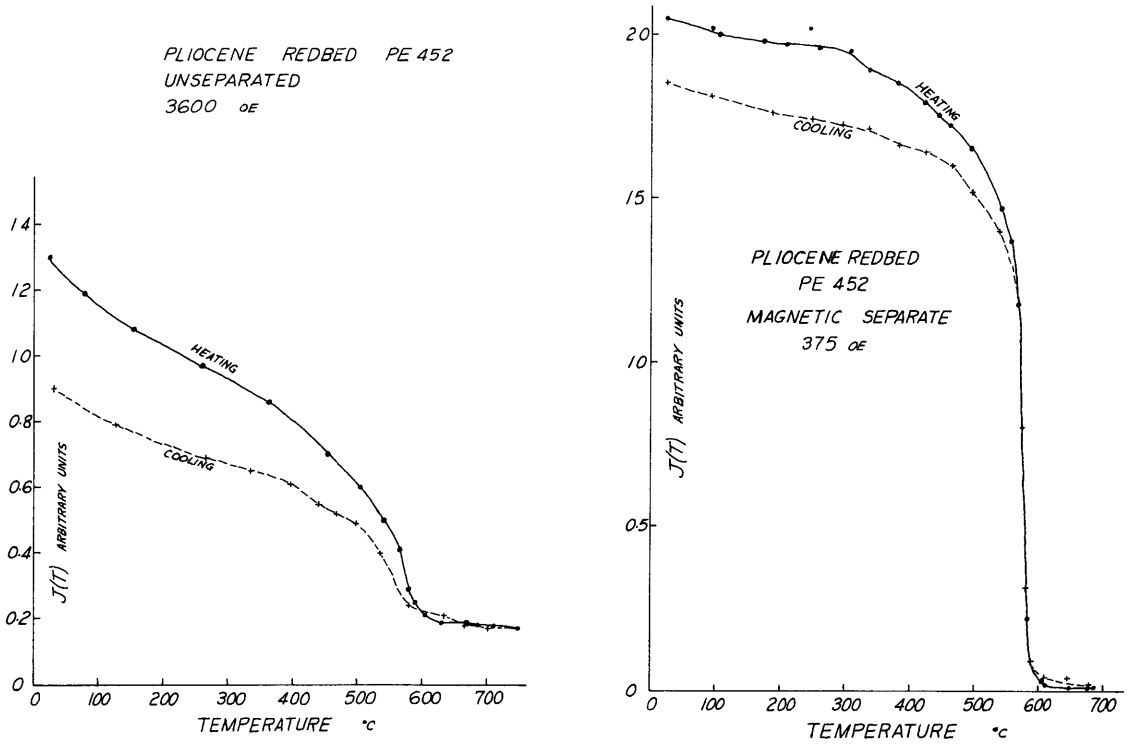
PLIOCENE REDBED PE 452
UNSEPARATED
3600 oE
HEATING
COOLING
J(T) ARBITRARY UNITS
TEMPERATURE °C
PLIOCENE REDBED
PE 452
MAGNETIC SEPARATE
375 oE
HEATING
COOLING
J(T) ARBITRARY UNITS
TEMPERATURE °C

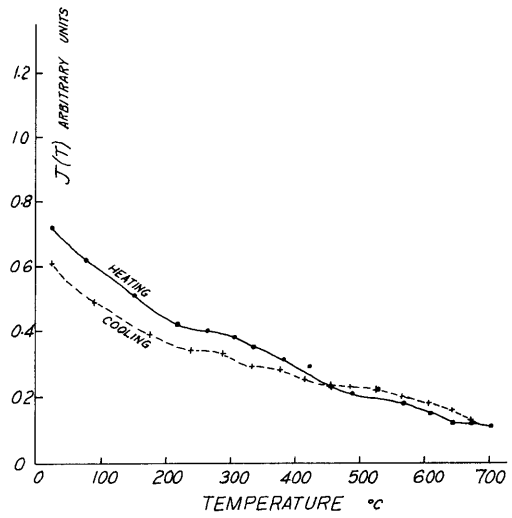
PLIOCENE REDBED PE 452
NON - MAGNETIC SEPARATE
5100 oE
J(T) ARBITRARY UNITS
HEATING
COOLING
TEMPERATURE °C

FIG. 22

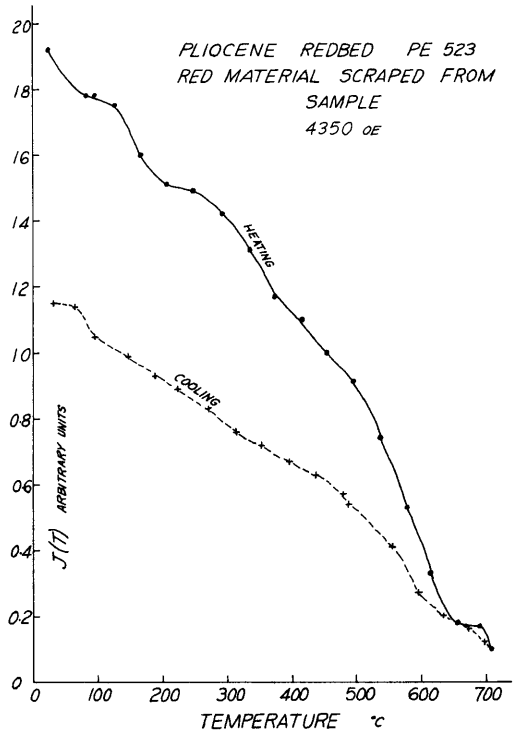
PLIOCENE REDBED PE 523
RED MATERIAL SCRAPED FROM
SAMPLE
4350 oE
HEATING
COOLING
J(T) ARBITRARY UNITS
TEMPERATURE °C

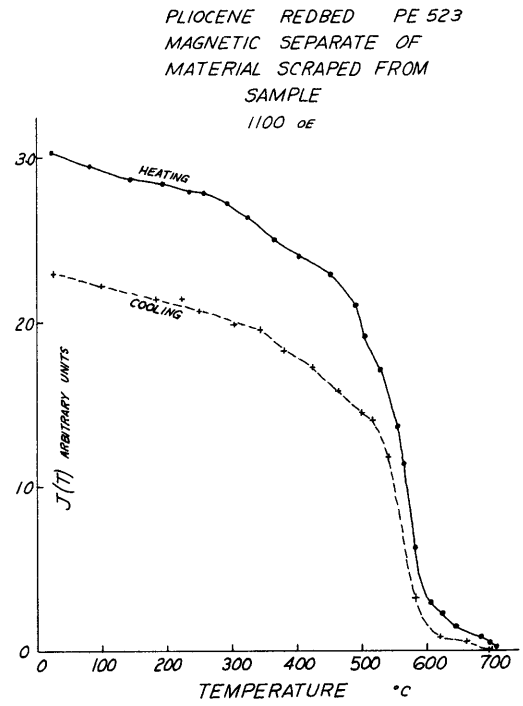
PLIOCENE REDBED PE 523
MAGNETIC SEPARATE OF
MATERIAL SCRAPED FROM
SAMPLE
1100 oE
HEATING
COOLING
J(T) ARBITRARY UNITS
TEMPERATURE °C

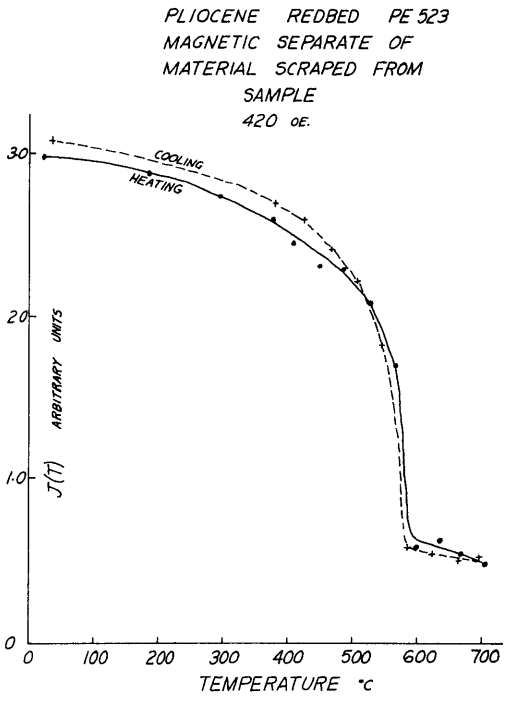
PLIOCENE REDBED PE 523
MAGNETIC SEPARATE OF
MATERIAL SCRAPED FROM
SAMPLE
420 oE.
COOLING
HEATING
J(T) ARBITRARY UNITS
TEMPERATURE °C

FIG.23

PLIOCENE REDBED PC27
MAGNETIC SEPARATE
275 OE

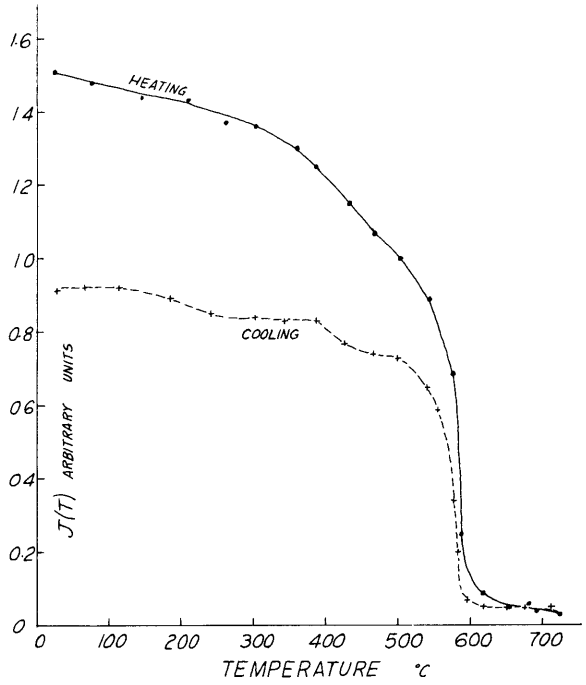

PLIOCENE REDBED PC 27
NON-MAGNETIC SEPARATE
510 OE

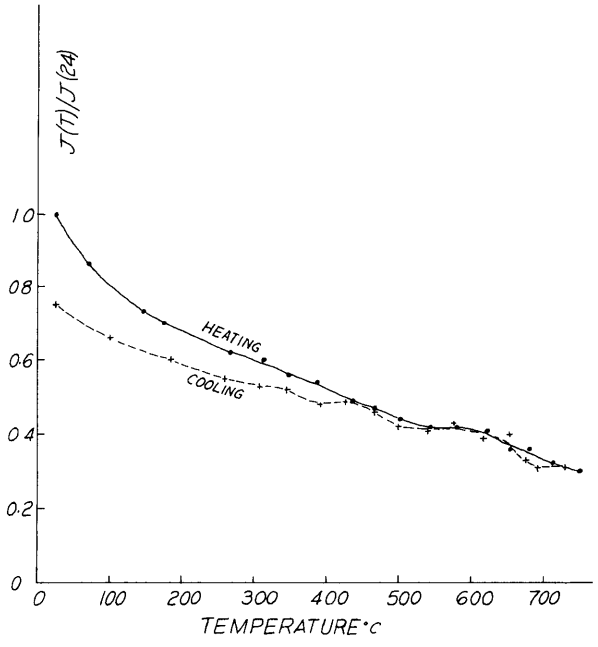

FIG. 24

PLIOCENE REDBED WF-RB-4
UNSEPARATED, < 2 μ FRACTION
3600 OE.

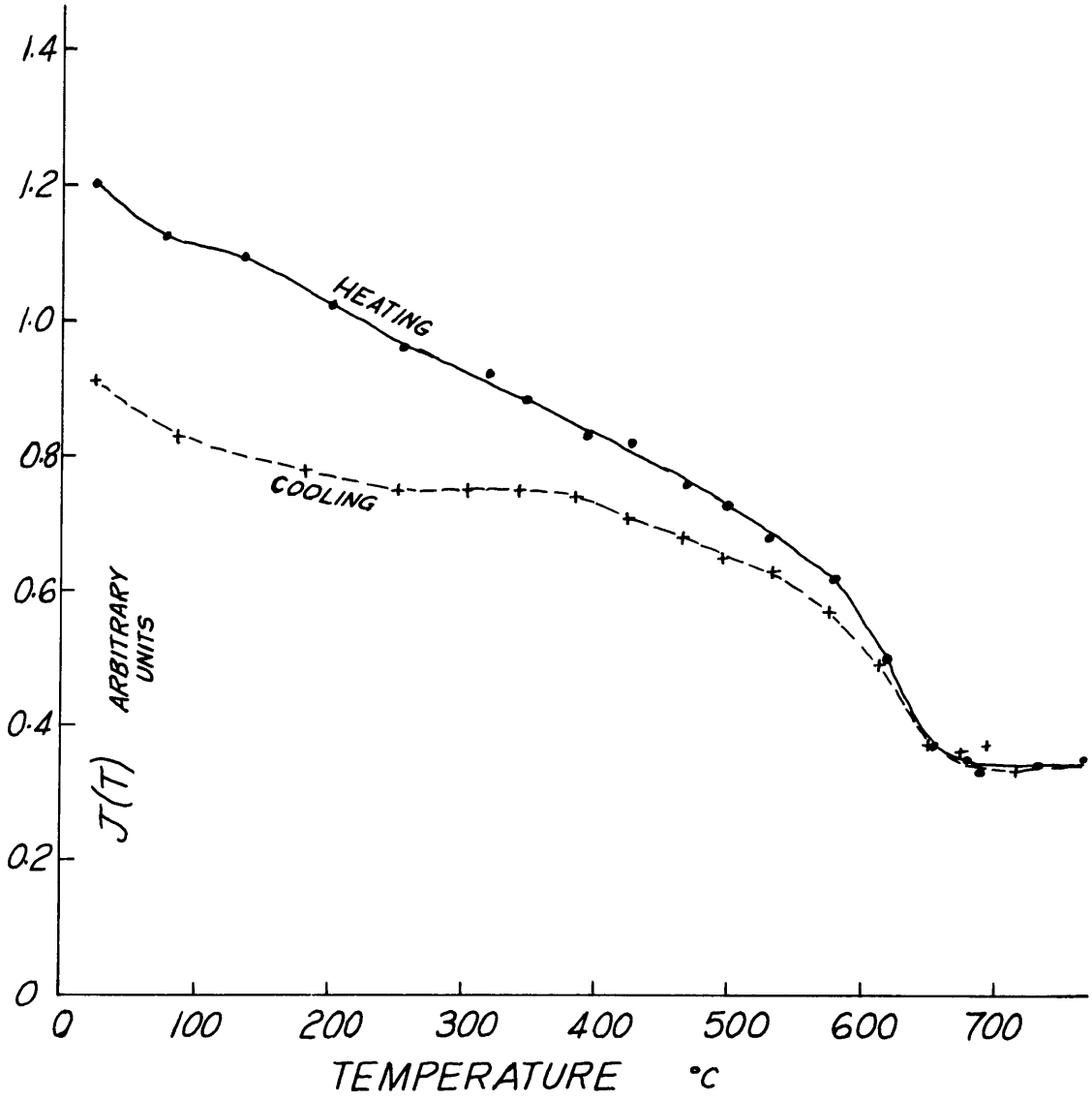

FIG. 25

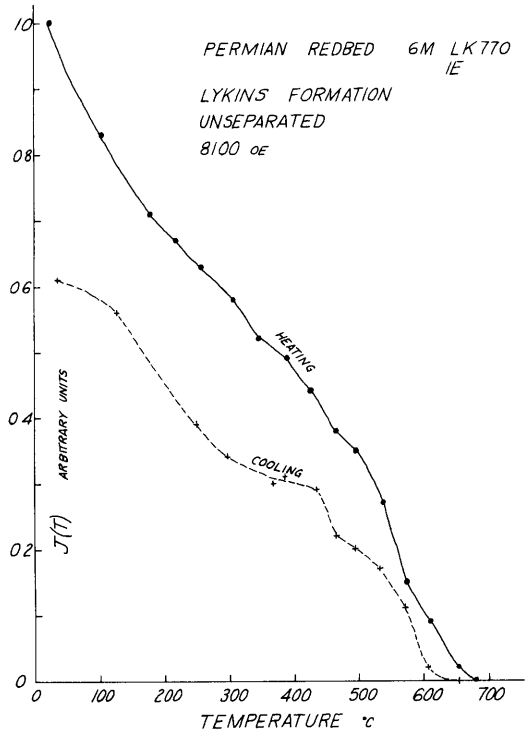
PERMIAN REDBED 6M LK770 IE
LYKINS FORMATION
UNSEPARATED
8100 oE
HEATING
COOLING
J(T) ARBITRARY UNITS
TEMPERATURE °C
0
02
04
06
08
10
0
100
200
300
400
500
600
700

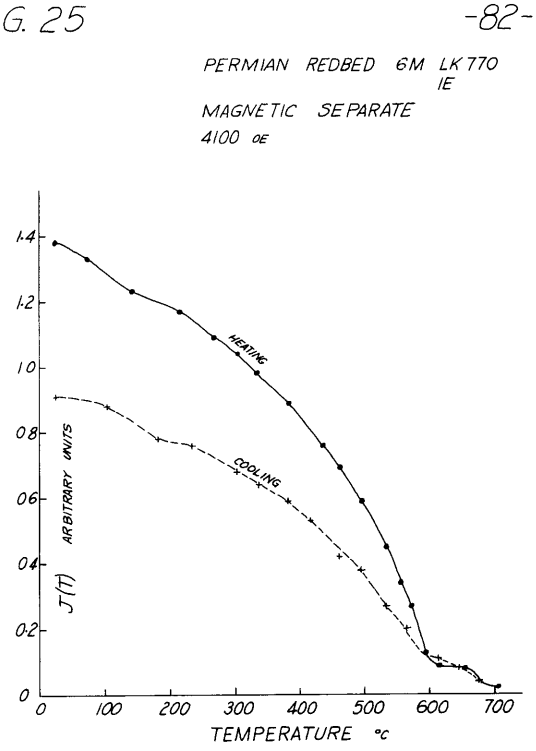
PERMIAN REDBED 6M LK770 IE
MAGNETIC SEPARATE
4100 oE
HEATING
COOLING
J(T) ARBITRARY UNITS
TEMPERATURE °C
0
02
04
06
08
10
12
14
0
100
200
300
400
500
600
700

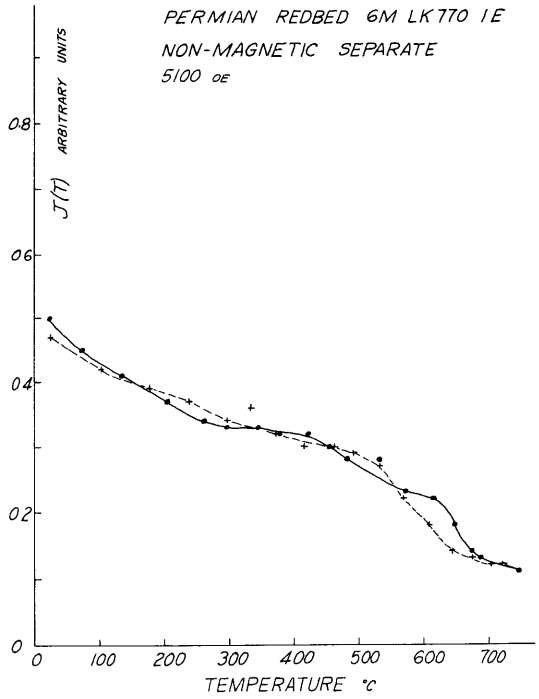
PERMIAN REDBED 6M LK770 IE
NON-MAGNETIC SEPARATE
5100 oE
J(T) ARBITRARY UNITS
TEMPERATURE °C
0
02
04
06
08
0
100
200
300
400
500
600
700

FIG. 26

PERMIAN REDBED LHR LK3
LYKINS FORMATION
MAGNETIC SEPARATE
1550 oE.

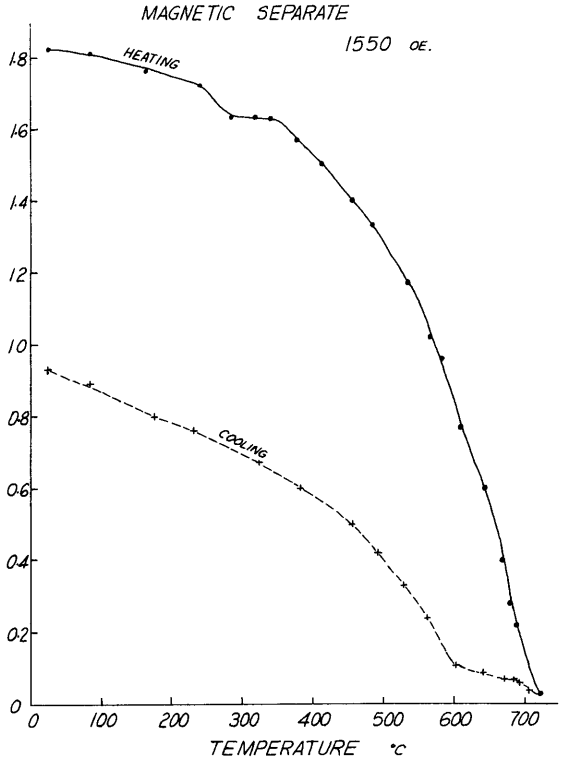

PERMIAN REDBED LHR LK3
NON-MAGNETIC SEPARATE
5100 oE

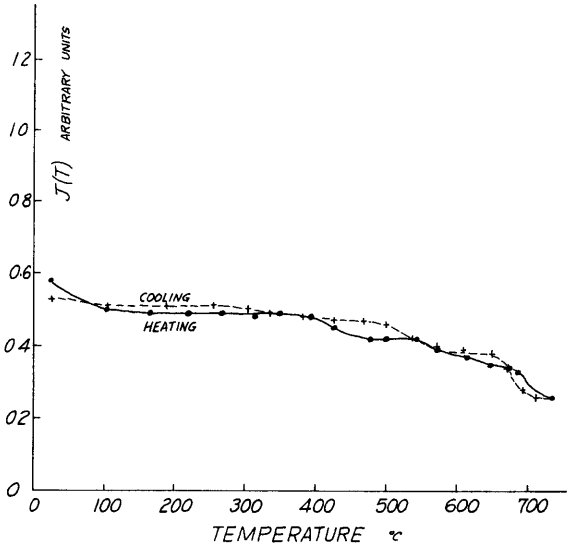

FIG. 27

PERMIAN REDBED 9891
LYONS FORMATION, ROCKY
MOUNTAIN ARSENAL WELL
MAGNETIC SEPARATE
660 OE.

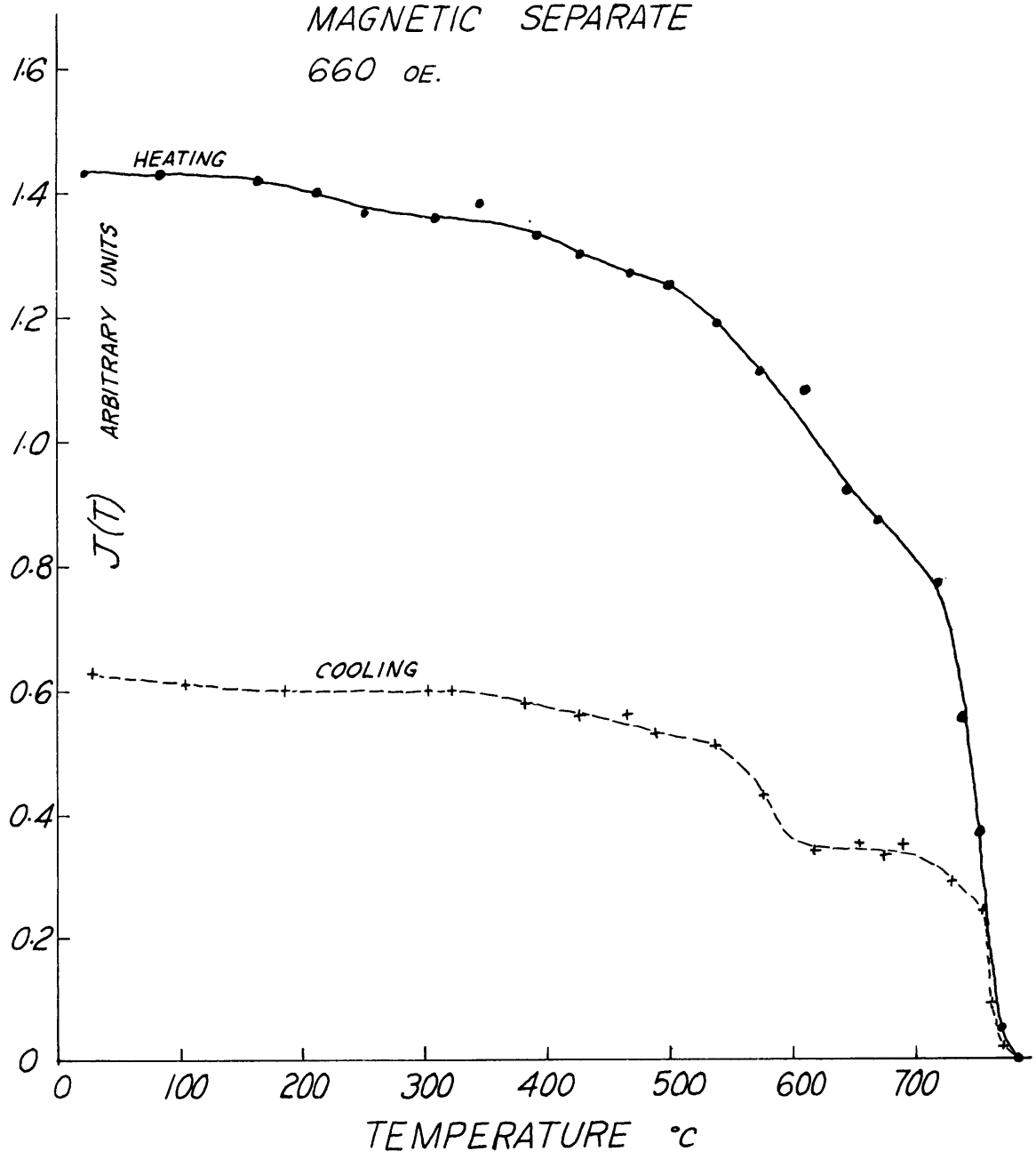

FIG. 28

PERMIAN REDBED DP E-2-0
INGLESIDE FORMATION
MAGNETIC SEPARATE
2500 OE.

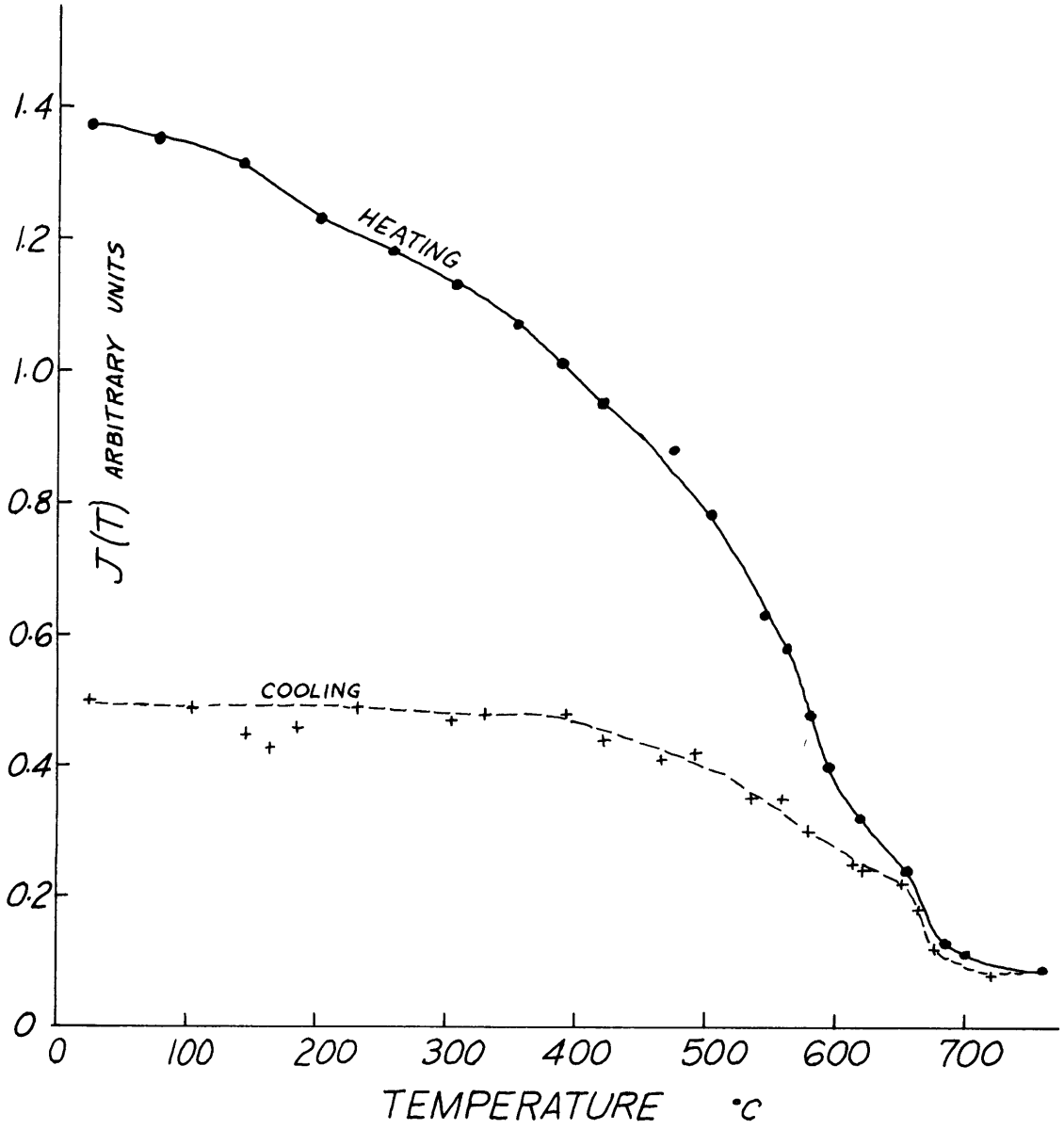

FIG. 29

PERMIAN REDBED FF 75·1
FOUNTAIN FORMATION
MAGNETIC SEPARATE
720 OE.

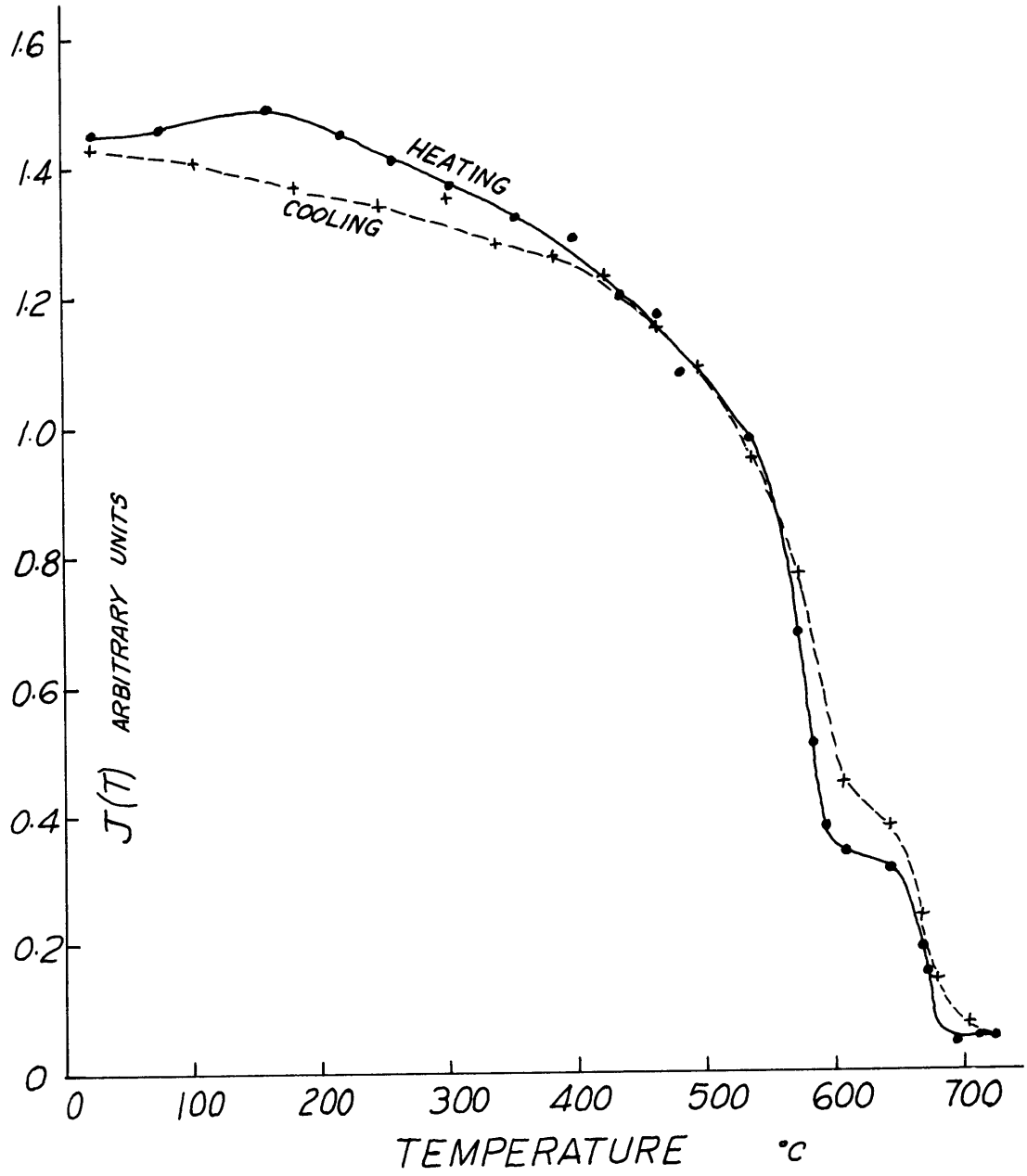

FIG. 30

PENNSYLVANIAN REDBED
RSC 880-2
MINTURN FORMATION
MAGNETIC SEPARATE
3050 OE.

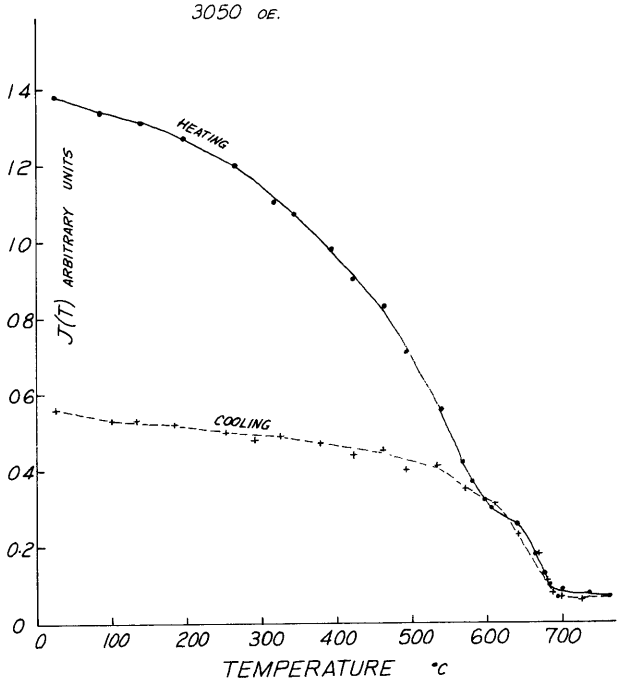

PENNSYLVANIAN REDBED
RSC 880-2
NON-MAGNETIC SEPARATE
5100 OE.